

# BROTOCs and Quantum Information Scrambling at Finite Temperature

Namit Anand and Paolo Zanardi

Department of Physics and Astronomy, and Center for Quantum Information Science and Technology, University of Southern California, Los Angeles, California 90089-0484, USA

June 16, 2022

**Out-of-time-ordered correlators (OTOCs)** have been extensively studied in recent years as a diagnostic of quantum information scrambling. In this paper, we study quantum information-theoretic aspects of the *regularized* finite-temperature OTOC. We introduce analytical results for the *bipartite regularized* OTOC (BROTOC): the regularized OTOC averaged over random unitaries supported over a bipartition. We show that the BROTOC has several interesting properties, for example, it quantifies the purity of the associated thermofield double state and the “operator purity” of the analytically continued time-evolution operator. At infinite-temperature, it reduces to one minus the operator entanglement of the time-evolution operator. In the zero-temperature limit and for nondegenerate Hamiltonians, the BROTOC probes the groundstate entanglement. By computing long-time averages, we show that the equilibration value of the BROTOC is intimately related to eigenstate entanglement. Finally, we numerically study the equilibration value of the BROTOC for various physically relevant Hamiltonian models and comment on its ability to distinguish integrable and chaotic dynamics.

## 1 Introduction

The thermalization of closed quantum systems has been a long standing puzzle in theoretical physics [1–4]. Recently, the notion of “information scrambling” as the underlying mechanism for thermalization has gained prominence. The idea is that complex quantum systems quickly disseminate localized information through the (nonlocal) degrees of freedom, making it inaccessible to any *local* probes to the system. The information is not lost, since the global evolution is still unitary, rather, it is encoded in nonlocal correlations across the system. A quantification of

this dynamical phenomena has initiated a rich discussion surrounding operator growth [5–11], eigenstate thermalization hypothesis (ETH) [12], quantum chaos [13, 14], among others; see also Refs. [15, 16] for a recent review. One of the central objects in this quantification are the so-called out-of-time-ordered correlators (OTOCs). The OTOC is usually defined as a four point function with unusual time-ordering [17, 18],

$$F_\beta(t) := \text{Tr} \left[ W_t^\dagger V^\dagger W_t V \rho_\beta \right], \quad (1)$$

where  $W_t := U_t^\dagger W U_t$  is the Heisenberg-evolved operator and  $\rho_\beta = \exp[-\beta H] / \mathcal{Z}(\beta)$  is the Gibbs state at inverse temperature  $\beta$  with  $\mathcal{Z}(\beta) := \text{Tr}[\exp[-\beta H]]$ . An intimately related quantity to the above OTOC is the following norm of the commutator,

$$\begin{aligned} C_\beta(t) &:= \frac{1}{2} \text{Tr} \left[ [W_t, V]^\dagger [W_t, V] \rho_\beta \right] \\ &= \frac{1}{2} \|[W_t, V] \sqrt{\rho_\beta}\|_2^2. \end{aligned} \quad (2)$$

Here we have used the Hilbert-Schmidt norm  $\|\cdot\|_2$ , which originates from the (Hilbert-Schmidt) inner product  $\langle A, B \rangle := \text{Tr}[A^\dagger B]$ . The two quantities are related via the simple formula,

$$C_\beta(t) = 1 - \text{Re}F_\beta(t). \quad (3)$$

Therefore, the growth of the norm of the commutator is associated to the decay of the OTOCs.

The idea behind using the norm of the commutator to quantify scrambling is the following: let  $V$  and  $W$  be two local operators that initially commute (for example, consider local operators on two different sites of a quantum spin-chain). Under Heisenberg time-evolution, the support of  $W_t$  grows and after a transient period, it will start noncommuting with the operator  $V$  and one can utilize the commutator  $C_\beta(t)$  to quantify this growth. Intuitively, if the Hamiltonian of this system is local, then Leib-Robinson type bounds can provide an estimate for the time it takes for the growth of this commutator [19–21].

Understanding quantitatively, the scrambling of quantum information has lead to a plethora of the-

Namit Anand: e-mail: [namitana@usc.edu](mailto:namitana@usc.edu)

Paolo Zanardi: e-mail: [zanardi@usc.edu](mailto:zanardi@usc.edu)

oretical insights [5–13, 22, 23]. This was swiftly followed by several state-of-the-art experimental investigations [24–33]. Furthermore, several works have now elucidated quantum information theoretic aspects underlying the OTOC, for example, by connecting it to Loschmidt Echo [34], operator entanglement and entropy production [35, 36], quantum coherence [37], entropic uncertainty relations [38], among others.

In Refs. [34, 35], the authors defined a “bipartite OTOC,” obtained by averaging the infinite-temperature OTOC uniformly over local random unitaries supported on a bipartition. In Ref. [35], this bipartite OTOC was shown to have the following operational interpretations: (i) it is exactly the *operator entanglement* [39, 40] of the dynamical unitary  $U_t$ , (ii) it connects in a simple way to the entangling power [41] of the dynamical unitary  $U_t$ , (iii) it is exactly equal to the average linear entropy production power of the reduced dynamics, among others. Furthermore, several of these connections were generalized to the case of open-system dynamics in Ref. [36], where, in particular, a competition between information scrambling and environmental decoherence was uncovered [42].

Unfortunately, as we move away from the infinite-temperature assumption, the connections unveiled in Ref. [35] do not carry over their operational aspects anymore. For example, a straightforward generalization to the finite temperature case, say, by using the OTOC as defined in Eq. (1) fails to retain the operator entanglement or entropy production connection. Not all is lost, however, as it is the *regularized* OTOC [13] that naturally lends itself to these operational connections. Elucidating this connection is the key technical contribution of this work. For ease of readability, the proofs of key Propositions appear in the Appendix.

## 2 Preliminaries

The OTOC introduced in Eq. (1) will hereafter be referred to as the *unregularized* OTOC. In contrast, the *regularized* (or symmetric) OTOC is defined as [13],

$$F_\beta^{(r)}(t) := \text{Tr} \left[ W_t^\dagger y V^\dagger y W_t y V y \right] \text{ with } y^4 = \rho_\beta. \quad (4)$$

Equivalently,

$$F_\beta^{(r)}(t) = \frac{1}{\mathcal{Z}(\beta)} \text{Tr} \left[ W_t^\dagger x V^\dagger x W_t x V x \right], \quad (5)$$

with  $x = \exp[-\beta H/4]$ . We also define the associated disconnected correlator [13],

$$F_\beta^{(d)}(t) := \text{Tr} \left[ \sqrt{\rho_\beta} W_t^\dagger \sqrt{\rho_\beta} W_t \right] \text{Tr} \left[ \sqrt{\rho_\beta} V^\dagger \sqrt{\rho_\beta} V \right]. \quad (6)$$

In Ref. [13], a bound on the growth of the correlator  $F_\beta^{(d)}(t) - F_\beta^{(r)}(t)$  was obtained under certain assumptions as

$$\frac{\partial}{\partial t} \log \left( F_\beta^{(d)}(t) - F_\beta^{(r)}(t) \right) \leq \frac{2\pi}{\beta}. \quad (7)$$

We also refer the reader to Ref. [12] the same bound was derived for systems satisfying ETH, along with some extra assumptions. In this work we focus on the quantity  $F_\beta^{(d)}(t) - F_\beta^{(r)}(t)$  arising from this bound and connect it to operational, quantum information-theoretic quantities. Notice that, for a time-independent Hamiltonian, the disconnected correlator  $F_\beta^{(d)}(t)$  is time independent (by using the commutation of  $[y^2, U_t]$  and the cyclicity of trace). Therefore, we can define,  $F_\beta^d \equiv F_\beta^{(d)}(t) = \text{Tr} [y^2 W^\dagger y^2 W] \text{Tr} [y^2 V^\dagger y^2 V]$ .

Following Ref. [35], we will consider the following setup: let  $\mathcal{H}_{AB} = \mathcal{H}_A \otimes \mathcal{H}_B \cong \mathbb{C}^{d_A} \otimes \mathbb{C}^{d_B}$  be a bipartition of the Hilbert space. Define as  $\mathcal{U}(\mathcal{H}_{A(B)})$ , the unitary group over  $\mathcal{H}_{A(B)}$ . We want to understand the qualitative and quantitative features of the OTOC for a *generic* choice of local operators  $V$  and  $W$ . Therefore, we average over unitary operators supported on the bipartition  $A|B$ . We define the bipartite averaged, *unregularized* OTOC (hereafter, bipartite unregularized OTOC) as [35]

$$G_\beta(t) := \mathbb{E}_{V_A, W_B} [C_\beta(t)], \quad (8)$$

where,  $V_A = V \otimes \mathbb{I}_B, W_B = \mathbb{I}_A \otimes W$ , with  $V \in \mathcal{U}(\mathcal{H}_A), W \in \mathcal{U}(\mathcal{H}_B)$ , and  $\mathbb{E}_{V, W} [\bullet] := \int_{\text{Haar}} dV dW [\bullet]$  denotes Haar-averaging over the standard uniform measure over  $\mathcal{U}(\mathcal{H}_{A(B)})$  [43]. In Ref. [35] it was shown that one can analytically perform the Haar averages to obtain the following expression,

$$G_\beta(t) = 1 - \frac{1}{d} \text{Re} \text{Tr} \left( (\rho_\beta \otimes \mathbb{I}_{A'B'}) U_t^{\dagger \otimes 2} \mathbb{S}_{AA'} U_t^{\otimes 2} \mathbb{S}_{AA'} \right), \quad (9)$$

where  $\mathbb{S}_{AA'}$  is the operator that swaps the  $A \leftrightarrow A'$  spaces in  $\mathcal{H}_A \otimes \mathcal{H}_B \otimes \mathcal{H}_{A'} \otimes \mathcal{H}_{B'}$ . This equation represents the finite temperature version of the unregularized bipartite OTOC. For  $\beta = 0$ , this is the operator entanglement of the time evolution operator  $U_t$  as will be discussed shortly. However, for  $\beta \neq 0$ , it does not have a clear quantum information-theoretic correspondence.

Ref. [35] studied  $G_\beta(t)$  in extensive detail at  $\beta = 0$ . Here, we will contrast the dynamical behavior of the bipartite unregularized OTOC with that of the regularized case, which we are now ready to introduce. Performing bipartite averages in a similar way for the

regularized case, we have,

$$N_\beta(t) := G_\beta^{(d)} - G_\beta^{(r)}(t), \quad (10)$$

$$\text{with } G_\beta^{(d)} := \mathbb{E}_{V_A, W_B} \left[ F_\beta^{(d)} \right], \quad (11)$$

$$\text{and } G_\beta^{(r)}(t) := \mathbb{E}_{V_A, W_B} \left[ F_\beta^{(r)}(t) \right]. \quad (12)$$

In the next section, we will discuss information-theoretic aspects of these quantities. We also refer the reader to Refs. [11, 44–48] for a discussion of various information scrambling/operator growth aspects of the regularized versus unregularized OTOCs.

*Operator Schmidt decomposition.*— We take a small detour to remind the reader a few key facts about operator entanglement before delving into our main results. Given a pure quantum state in a bipartite Hilbert space,  $|\psi\rangle \in \mathcal{H} \cong \mathcal{H}_A \otimes \mathcal{H}_B$ , there exists a Schmidt decomposition of this state [49],

$$|\psi\rangle = \sum_{j=1}^r \sqrt{\lambda_j} |j_A\rangle \otimes |j_B\rangle. \quad (13)$$

Here,  $\{\lambda_j\}_j$  are nonnegative coefficients with  $r = \min(d_A, d_B)$  the Schmidt rank and  $\{|j_A\rangle\}_{j=1}^{d_A}$ ,  $\{|j_B\rangle\}_{j=1}^{d_B}$  bases for the subsystems  $A, B$ , respectively. The Schmidt coefficients can be used to compute various entanglement measures for the bipartite state  $|\psi\rangle$  [50]. The key idea behind Schmidt decomposition is to use the singular value decomposition for the matrix of coefficients obtained from expressing the state  $|\psi\rangle$  with respect to local orthonormal bases. In fact, one can generalize this idea to the operator space. Namely, consider bipartite operators, i.e., elements of  $\mathcal{L}(\mathcal{H}_A \otimes \mathcal{H}_B)$ , then we can define an *operator Schmidt decomposition* [39, 51, 52]. Formally, given a bipartite operator  $X \in \mathcal{L}(\mathcal{H}_A \otimes \mathcal{H}_B)$ , there exist orthogonal bases  $\{U_j\}_{j=1}^{d_A^2}$  and  $\{W_j\}_{j=1}^{d_B^2}$  for  $\mathcal{L}(\mathcal{H}_A), \mathcal{L}(\mathcal{H}_B)$ , respectively, such that  $\langle U_j, U_k \rangle = d_A \delta_{jk}$  and  $\langle W_j, W_k \rangle = d_B \delta_{jk}$ . Moreover,

$$X = \sum_{j=1}^{\tilde{r}} \sqrt{\lambda_j} U_j \otimes W_j. \quad (14)$$

The coefficients  $\{\lambda_j\}_j$  are nonnegative and are called the operator Schmidt coefficients and  $\tilde{r} = \min\{d_A^2, d_B^2\}$  is the operator Schmidt rank. In fact, the operator entanglement of a unitary introduced in Ref. [39] is exactly the linear entropy of the probability vector  $\vec{p} = (\lambda_1, \lambda_2, \dots, \lambda_{\tilde{r}})$  arising from the operator Schmidt coefficients. A key result obtained in Ref. [39] was that the operator entanglement of a unitary operator can be equivalently expressed as,

$$E_{\text{op}}(U) = 1 - \frac{1}{d^2} \text{Tr} [\mathbb{S}_{AA'} U^{\otimes 2} \mathbb{S}_{AA'} U^{\dagger \otimes 2}]. \quad (15)$$

In a similar spirit, we define the *operator purity* of a linear operator as the purity of the probability vector

$\vec{p}$  obtained following the operator Schmidt decomposition. Namely,

$$\mathcal{P}_{\text{op}}(X) := \frac{1}{\|X\|_2^4} \text{Tr} [\mathbb{S}_{AA'} X^{\otimes 2} \mathbb{S}_{AA'} X^{\dagger \otimes 2}], \quad (16)$$

where we have explicitly introduced the normalization  $\|X\|_2^4$  for arbitrary operators (it is equal to  $d^2$  for unitaries which recovers the previous formula above).

Lastly, we remind the reader that, for unitary dynamics, information scrambling is usually quantified via the OTOCs, the operator entanglement of the time-evolution operator  $U_t$ , and the quantum mutual information [23]. Our work, in particular, focuses extensively on the interplay between OTOCs and operator entanglement.

### 3 Main results

#### 3.1 Operator entanglement

Our first result is to bring  $N_\beta(t)$  into an exact analytical form. We introduce some notation first. Let  $\mathcal{P}_\chi(\rho) := \|\rho_\chi\|_2^2$  be the squared 2-norm of the operator  $\rho_\chi$  with  $\rho_\chi := \text{Tr}_{\bar{\chi}}[\rho]$ ,  $\chi = \{A, B\}$ , and  $\bar{\chi}$  the complement of  $\chi$ . If  $\rho$  is a quantum state then  $\mathcal{P}_\chi(\rho)$  is the purity across the  $A|B$  partition.

**Proposition 1.** *The regularized bipartite OTOC at finite temperature is*

$$\begin{aligned} N_\beta(t) = & \frac{1}{d} \mathcal{P}_A(\sqrt{\rho_\beta}) \mathcal{P}_B(\sqrt{\rho_\beta}) \\ & - \frac{1}{d \mathcal{Z}_\beta} \text{Tr} [\mathbb{S}_{AA'} \mathcal{U}_{\beta,t}^{\otimes 2} (\mathbb{S}_{AA'})], \end{aligned} \quad (17)$$

where,  $\mathcal{U}_{\beta,t} := \mathcal{V}_\beta \circ \mathcal{U}_t$  with  $\mathcal{V}_\beta(X) := \exp[-\beta H/4] X \exp[-\beta H/4]$  the imaginary time-evolution,  $\mathcal{U}_t(X) := U_t^\dagger X U_t$  the real time-evolution, and  $U_t = \exp[-iHt]$  the usual time-evolution operator.

Let us note a few simple things about this result: (i) at infinite temperature ( $\beta = 0$ ), this reduces to the operator entanglement of the time evolution operator [35]  $G_{\beta=0}(t)$ . The equilibration value of this quantity was used to distinguish various integrable and chaotic models, see Refs. [35, 53] for more details. (ii) In quantum information theory [49], the most general description of the dynamics of a quantum system is given by a completely positive (CP) and trace-nonincreasing map, also called a *quantum operation*. Furthermore, if the evolution is not only trace non-increasing, rather, trace-preserving (TP), then such dynamical maps are called *quantum channels*. In the Appendix, we show that  $\mathcal{U}_{\beta,t}$  is a quantum operation. Moreover, the second term,  $G_\beta^{(r)}(t)$  is real and proportional to the operator purity of

$U_\beta(t) := \exp[-(\beta - it)H/4]$ , the analytically continued time-evolution operator, with  $\mathcal{Z}(\beta/2)^2 / (d\mathcal{Z}(\beta))$  as the proportionality factor. (iii) The following simple upper bound holds for the BROTOC:  $N_\beta(t) = G_\beta^{(d)} - G_\beta^{(r)}(t) \leq G_\beta^{(d)} \leq \mathcal{Z}(\beta/2)^4 / (d\mathcal{Z}(\beta)^2)$ . (iv) For a non-entangling Hamiltonian, we have,  $N_\beta = 0 \ \forall \beta$ . Namely, if  $H = H_A + H_B$ , then a simple calculation reveals that,  $G_\beta^{(d)} = \frac{\mathcal{Z}(\beta/2)^2}{d\mathcal{Z}(\beta)} = G_\beta^{(r)}$  and therefore,  $N_\beta(t)$  is identically vanishing at all  $\beta$ . Of course, the fact that at  $\beta = 0$ ,  $N_\beta = 0$  also follows from the connection to operator entanglement [35].

We emphasize that, although several previous works have focussed on understanding the growth of local OTOCs in terms of Lieb-Robinson bounds [54–59], this analysis *does not* apply to our bipartite OTOCs (regularized or unregularized). The key distinction here is that, our averaging is over observables supported on a bipartition  $A|B$  of the *entire* system (and not some subset of the total Hilbert space). As a result, even if one of the subsystems is local its complement is (highly) nonlocal. As a result, Lieb-Robinson type bounds are not necessarily useful in understanding the growth of this quantity.

### 3.2 BROTOC, thermofield double, and the spectral form factor

In this section, we focus on the quantum operation  $\mathcal{U}_{\beta,t}$ , the operator purity of which is quantified by the connected BROTOC. We will show that the map  $\mathcal{U}_{\beta,t}$  contains information about both spectral and eigenstate signatures of quantum chaos [3, 60–62]. In particular, we will establish its relation to the spectral form factor (SFF) [63] and the thermofield double state (TDS) [64]. Recently, several works have elucidated the ability of the TDS to probe scrambling and quantum chaos [22, 65–67]. In its simplest form, the TDS corresponds to a “canonical” purification of the Gibbs state  $\rho_\beta = \exp[-\beta H] / \mathcal{Z}(\beta)$ . Given the connections to scrambling and chaos, the ability to experimentally prepare TDS allows us to directly probe these properties; see for e.g., Refs. [68–72] for a discussion about how to prepare such states on a quantum computer.

More formally, let  $|\Gamma\rangle := \sum_{j=1}^d |j\rangle|j\rangle$  be the *unnormalized* maximally entangled vector in  $\mathcal{H}^{\otimes 2}$ , then, the TDS is defined as,

$$|\psi(\beta)\rangle := (\sqrt{\rho_\beta} \otimes \mathbb{I}) |\Gamma\rangle. \quad (18)$$

By construction,  $|\psi(\beta)\rangle \in \mathcal{H}^{\otimes 2}$  and tracing out either subsystem gives us back the original Gibbs state. For simplicity, consider a nondegenerate Hamiltonian with a spectral decomposition  $H = \sum_{j=1}^d E_j |j\rangle\langle j|$ , then, by considering the  $|\Gamma\rangle$  matrix expressed with respect

to the Hamiltonian eigenbasis, we have,

$$|\psi(\beta)\rangle = \frac{1}{\sqrt{\mathcal{Z}(\beta)}} \sum_{j=1}^d \exp[-\beta E_j/2] |j\rangle|j\rangle. \quad (19)$$

Written in this form, it is easy to see that partial tracing either subsystem of  $|\psi(\beta)\rangle$  generates the Gibbs state  $\rho_\beta$ . In Ref. [66], the survival probability (or Loschmidt Echo) of the time-evolving TDS was related to the analytically continued partition function [13, 22, 65]. Namely, let the time-evolved TDS be defined as [64, 66],

$$\begin{aligned} |\psi(\beta, t)\rangle &:= (U_t \otimes \mathbb{I}) |\psi(\beta)\rangle \\ &= \frac{1}{\sqrt{\mathcal{Z}(\beta)}} \sum_{j=1}^d \exp[-(\beta/2 + it)E_j] |j\rangle|j\rangle, \end{aligned} \quad (20)$$

then its survival probability is

$$|\langle\psi(\beta, 0)|\psi(\beta, t)\rangle|^2 = \frac{|\mathcal{Z}(\beta + it)|^2}{\mathcal{Z}(\beta)^2}. \quad (21)$$

This is clearly related to the two-point, analytically continued SFF, which is defined as [22, 73],

$$\mathcal{R}_2(\beta, t) := \langle |\mathcal{Z}(\beta + it)|^2 \rangle_{\text{RMT}}, \quad (22)$$

where  $\langle \dots \rangle_{\text{RMT}}$  denotes an ensemble average, usually over a random matrix ensemble of Hamiltonians [61].

We will now show that an analogous, though, not identical, result holds for the quantum operation  $\mathcal{U}_{\beta,t}$ . Namely, we will consider the fidelity between the Choi-Jamiolkowski (CJ) matrix [74] corresponding to  $\mathcal{U}_{\beta,t}$  and  $\mathcal{U}_{\beta,0}$  and show that it is related to the two-point SFF. Recall that the Choi-Jamiolkowski isomorphism is an isomorphism between linear maps  $\mathcal{E} : \mathcal{L}(\mathcal{H}) \rightarrow \mathcal{L}(\mathcal{K})$  to matrices  $\rho_\mathcal{E} \in \mathcal{L}(\mathcal{H}) \otimes \mathcal{L}(\mathcal{K})$  [74]. Let  $|\phi^+\rangle := \frac{1}{\sqrt{d}} |j\rangle|j\rangle$  be the *normalized* maximally entangled state in  $\mathcal{H}^{\otimes 2}$ , then,

$$\rho_\mathcal{E} := \mathcal{E} \otimes \mathcal{I} (|\phi^+\rangle\langle\phi^+|). \quad (23)$$

A linear map  $\mathcal{E}$  is CP  $\iff \rho_\mathcal{E} \geq 0$ . Now, a simple calculation shows that the CJ matrix corresponding to the quantum operation  $\mathcal{U}_{\beta,t}$  is,

$$\rho_{\mathcal{U}_{\beta,t}} = \frac{\mathcal{Z}(\beta/2)}{d} |\psi(\beta/2, t)\rangle\langle\psi(\beta/2, t)|. \quad (24)$$

To quantify how close two pure quantum states are, we can compute the fidelity [49] between them. Recall that the fidelity between two pure quantum states  $|\psi\rangle, |\phi\rangle$  is given as,

$$F(|\psi\rangle, |\phi\rangle) = |\langle\psi|\phi\rangle|^2, \quad (25)$$

with  $F(|\psi\rangle, |\phi\rangle) = 1 \iff |\psi\rangle = |\phi\rangle$ . Since the Choi matrix  $\rho_{\mathcal{U}_{\beta,t}}$  is proportional to a pure-state projector,

the fidelity between the matrices  $\rho_{\mathcal{U}_{\beta,t}}$  and  $\rho_{\mathcal{U}_{\beta,0}}$  can be defined as,

$$\begin{aligned} F(\rho_{\mathcal{U}_{\beta,t}}, \rho_{\mathcal{U}_{\beta,0}}) &\equiv \left( \frac{\mathcal{Z}(\beta/2)}{d} \right)^2 F(|\psi(\beta/2, t)\rangle, |\psi(\beta/2, 0)\rangle) \\ &= \left( \frac{\mathcal{Z}(\beta/2)}{d} \right)^2 |\langle\psi(\beta/2, t)|\psi(\beta/2, 0)\rangle|^2 \\ &= \frac{\mathcal{R}_2^H(\beta/2, t)}{d^2}, \end{aligned} \quad (26)$$

where  $\mathcal{R}_2^H$  is the two-point SFF *before* ensemble averaging [73], analogous to the result obtained in Ref. [66].

The above result connecting the quantum operation  $\mathcal{U}_{\beta,t}$  to the two-point SFF makes one wonder if a direct relation between the SFF and the regularized OTOC can be obtained, since the  $\mathcal{U}_{\beta,t}$  originates in the choice of the regularization for the thermal OTOC [13]. We will now show that the regularized OTOC, averaged over *global* random unitaries is related to the *four-point* SFF. Notice that, unlike the bipartite averaging that we will focus on throughout this paper, this relies on *global* averages over the unitary group. The necessity of performing global averages to connect with SFF subtly hints at the nonlocality (in both space and time) of the SFF, see Refs. [22, 73] for a detailed discussion. Let

$$F_{\beta}^{(A,B,C,D)}(t) := \text{Tr}[yA_tyByC_tyD] \quad (27)$$

with  $y = \rho_{\beta}^{1/4}$ , then we have the following result.

**Proposition 2.** *The regularized four-point OTOC averaged globally over Haar-random unitaries is related to the four-point spectral form factor as,  $\mathbb{E}_{A_1, B_1, A_2 \in \mathcal{U}(\mathcal{H})} [F_{\beta}^{(A_1, B_1, A_2, B_2)}(t)] = \mathcal{R}_4^{(H)}(\beta/4, t) / (d^3 \mathcal{Z}(\beta))$ , where  $B_2 = A_2^\dagger B_1^\dagger A_1^\dagger$  and  $\mathcal{R}_4^{(H)}(\beta, t) := (\mathcal{Z}_{\beta}(t) \mathcal{Z}_{\beta}(t)^*)^2$  with  $\mathcal{Z}_{\beta}(t) = \text{Tr}[\exp[(-\beta + it)H]]$ , the analytically continued partition function.*

Moreover, notice that this formula can be easily generalized to the case of different regularizations of the OTOC, for example, if we have 2-point functions with  $\sqrt{\rho_{\beta}}$  inserted between them, then we can get the  $\mathcal{R}_2(\beta/2, t)$ . In the most general case, if we have,  $2k$ -point thermally regulated OTOCs (which will have  $\rho_{\beta}^{1/2k}$  inserted between them), then, this will connect with  $\mathcal{R}_{2k}(\beta/2k, t)$ .

*Purity of the thermofield double.*— We are now ready to focus again on the local properties that are quantified by the BROTOC. Let us consider a bipartition of the original Hilbert space,  $\mathcal{H} \cong \mathcal{H}_A \otimes \mathcal{H}_B$ . Then the Choi matrix corresponding to the CP map  $\mathcal{U}_{\beta,t}$  is a four-partite state, since  $\rho_{\mathcal{U}_{\beta,t}} \in \mathcal{L}(\mathcal{H}_A \otimes \mathcal{H}_B) \otimes$

$\mathcal{L}(\mathcal{H}_{A'} \otimes \mathcal{H}_{B'})$ , where the primed Hilbert spaces represent a replica of the original Hilbert space. We can then compute the 2-norm squared of the reduced Choi matrix  $\rho_{\mathcal{U}_{\beta,t}}^{AA'} \equiv \text{Tr}_{BB'}[\rho_{\mathcal{U}_{\beta,t}}]$  (or the purity if the matrix was normalized; it is already positive semidefinite). Then, a key lemma from Ref. [39] shows that  $\left\| \rho_{\mathcal{U}_{\beta,t}}^{AA'} \right\|_2^2 = \frac{1}{d^2} \text{Tr}[\mathbb{S}_{AA'} \mathcal{U}_{\beta,t}^{\otimes 2}(\mathbb{S}_{AA'})]$ . Therefore, the (connected component of the) regularized OTOC,

$$G_{\beta}^{(r)}(t) = \frac{d}{\mathcal{Z}(\beta)} \left\| \rho_{\mathcal{U}_{\beta,t}}^{AA'} \right\|_2^2. \quad (28)$$

That is, it is proportional to the 2-norm squared of the reduced Choi matrix for the quantum operation  $\mathcal{U}_{\beta,t}$ .

Now, let  $\mathcal{P}_{AA'}(|\psi\rangle_{ABA'B'}) := \left\| \text{Tr}_{BB'}[|\psi\rangle\langle\psi|_{ABA'B'}] \right\|_2^2$  be the purity of the thermofield double across the  $AA'|BB'$  partition. Then, using the fact that the Choi matrix of  $\mathcal{U}_{\beta,t}$  is proportional to the time-evolved thermofield double state  $|\psi(\beta/2, t)\rangle\langle\psi(\beta/2, t)|$ , we have,

$$G_{\beta}^{(r)}(t) = \frac{\mathcal{Z}(\beta/2)^2}{d\mathcal{Z}(\beta)} \mathcal{P}_{AA'}(|\psi(\beta/2, t)\rangle_{ABA'B'}). \quad (29)$$

Finally, notice that Page scrambling of a quantum state [23, 75, 76] is defined as all subsystems containing less than half the degrees of freedom being nearly maximally mixed. Since the purity is minimal for maximally mixed states, the closer the value of  $G_{\beta}^{(r)}(t)$  to the lower bound  $\frac{\mathcal{Z}(\beta/2)^2}{dd_A^2 \mathcal{Z}(\beta)}$ , the more information scrambling we have in the system's dynamics. That is, the connected component of the BROTOC quantifies the degree of Page scrambling in the time-evolving TDS. Furthermore, the connection to the purity of the thermofield double immediately allows us to infer the following bounds (which also follow from the connection to operator purity above),

$$\frac{\mathcal{Z}(\beta/2)^2}{dd_A^2 \mathcal{Z}(\beta)} \leq G_{\beta}^{(r)}(t) \leq \frac{\mathcal{Z}(\beta/2)^2}{d\mathcal{Z}(\beta)}, \quad (30)$$

where we have used the fact that the purity of a quantum state in  $\mathcal{H}_{AA'}$  is bounded between  $\frac{1}{d_A^2}$  and 1.

*Non-Hermitian evolution.*— The connected BROTOC has the form

$$G_{\beta}^{(r)}(t) = \frac{1}{d\mathcal{Z}(\beta)} \left\langle \mathbb{S}_{AA'}, \mathcal{U}_{\beta,t}^{\otimes 2}(\mathbb{S}_{AA'}) \right\rangle, \quad (31)$$

which quantifies the autocorrelation function between the observable  $\mathbb{S}_{AA'}$  and its evolved version  $\mathcal{U}_{\beta,t}^{\otimes 2}(\mathbb{S}_{AA'})$ . Now, recall that a non-Hermitian Hamiltonian is usually defined to be of the form,  $H = H_0 - i\Gamma$ , where  $H_0, \Gamma$  are Hermitian operators and we have separated the Hermitian and non-Hermitian parts explicitly. Assume that we are in the simple scenario where the Hermitian and anti-Hermitian parts

commute, namely,  $[H_0, \Gamma] = 0$ . Therefore, the time-evolution of an observable  $X$  under such dynamics is given as  $X_t = e^{-\Gamma t} e^{iH_0 t} X e^{-iH_0 t} e^{-\Gamma t}$ . For the connected BROTOC, if we identify  $\Gamma = \beta H/(4t)$  at  $t > 0$ , then we can think of  $\mathcal{U}_{\beta,t}$  as a simple *non-Hermitian* evolution (and the commutation assumption above is trivially satisfied). In this case, the BROTOC quantifies the scrambling power of non-Hermitian dynamics. This identification opens up the possibility of utilizing tools from the theory of dissipative quantum chaos [77–83] such as complex spacing ratios[83], to analyze directly the spectral correlations encoded in the non-Hermitian dynamics  $\mathcal{U}_{\beta,t}$  as a means of distinguishing integrable and chaotic dynamics. Furthermore, the ability to distinguish quantum chaos from decoherence is a fascinating question with a long history [60, 84]. Rewriting the quantum operation  $\mathcal{U}_{\beta,t} = \mathcal{V}_\beta \circ \mathcal{U}_t$  as a composition of a quantum operation  $\mathcal{V}_\beta$  (which signifies decoherence) and the unitary dynamics  $\mathcal{U}_t$  may allow for disentangling the decoherence effects from the *unitary scrambling*.

### 3.3 Zero-temperature limit

As we discussed above, the infinite-temperature limit of  $N_\beta(t)$  is the operator entanglement of the unitary  $U_t$  and enjoys several information-theoretic connections [35]. What about the other limit, namely,  $\beta \rightarrow \infty$ ? Here, we show that in the zero-temperature limit, the regularized OTOC probes the operator purity of the ground state projector, depending on the degeneracy of the ground state manifold. Let  $\Pi_0$  be the groundstate projector, then, recall that,  $\lim_{\beta \rightarrow \infty} \rho_\beta \rightarrow \Pi_0/g_0$ , where  $g_0$  is the groundstate degeneracy. That is, at zero temperature, the Gibbs state is proportional to the projector onto the groundstate manifold. Moreover, since  $\Pi_0$  is a projector, we have,  $\Pi_0^2 = \Pi_0$ . Therefore, the disconnected correlator simplifies to,

$$F_{\beta \rightarrow \infty}^{(d)} = \frac{1}{g_0^2} \text{Tr} [\Pi_0 V^\dagger \Pi_0 V] \text{Tr} [\Pi_0 W^\dagger \Pi_0 W]. \quad (32)$$

Similarly, for the regularized part we have,

$$F_{\beta \rightarrow \infty}^{(r)}(t) = \frac{1}{g_0} \text{Tr} [\Pi_0 W_t^\dagger \Pi_0 V^\dagger \Pi_0 W_t \Pi_0 V]. \quad (33)$$

Now, let  $H = \sum_j E_j \Pi_j$  be the spectral decomposition of the Hamiltonian, then, the projectors  $\{\Pi_j\}_j$  are orthonormal (but not necessarily rank-1). Plugging in  $U_t = \sum_j \exp[-iE_j t] \Pi_j$ , we get,

$$F_{\beta \rightarrow \infty}^{(r)}(t) = \frac{1}{g_0} \text{Tr} [\Pi_0 W^\dagger \Pi_0 V^\dagger \Pi_0 W \Pi_0 V]. \quad (34)$$

Now, if the groundstate is nondegenerate, then, we have,  $\Pi_0 = |\psi_{\text{gs}}\rangle\langle\psi_{\text{gs}}|$ , where  $|\psi_{\text{gs}}\rangle$  is the ground state

wavefunction and  $g_0 = 1$ . Then, a simple calculation shows that, for this case,

$$F_\beta^{(d)} = |\langle\psi_{\text{gs}}|V|\psi_{\text{gs}}\rangle|^2 |\langle\psi_{\text{gs}}|W|\psi_{\text{gs}}\rangle|^2 = F_\beta^{(r)} \quad (35)$$

and therefore, their difference vanishes. In fact, notice that, the four-point correlator has now reduced to a product of 1-point correlators. In summary, at zero temperature, for nondegenerate Hamiltonians, the correlator  $F_\beta^{(d)} - F_\beta^{(r)}(t)$  vanishes, and so does the regularized bipartite OTOC  $N_{\beta \rightarrow \infty}(t)$ .

We now perform the bipartite averaging for the zero-temperature case, without the assumption of nondegeneracy. The following result establishes that if the ground state is degenerate, then, both the disconnected and connected components of the regularized bipartite OTOC probe the entanglement in the ground state projector. Moreover, for the nondegenerate case, both terms are proportional to the square of the purity of the ground state and can be utilized to detect quantum phase transitions [85]. The ability of groundstate OTOCs to detect quantum phase transitions was explored in Ref. [86]. Establishing a possible connection to finite-temperature phase transitions is an interesting question for future investigations.

**Proposition 3.** *The disconnected and connected components of the bipartite averaged OTOC at zero temperature are,*

$$\begin{aligned} G_{\beta \rightarrow \infty}^{(d)} &= \frac{1}{dg_0^2} \mathcal{P}_A(\Pi_0) \mathcal{P}_B(\Pi_0), \text{ and} \\ G_{\beta \rightarrow \infty}^{(r)} &= \frac{1}{dg_0} \text{Tr} [\mathbb{S}_{AA'} \Pi_0^{\otimes 2} \mathbb{S}_{AA'} \Pi_0^{\otimes 2}]. \end{aligned} \quad (36)$$

Note that both quantities becomes *time-independent* and the convergence to the groundstate is *exponential* in  $\beta$ , given the Gibbs weights. Finally, we note that for a pure quantum state  $\Pi = |\psi\rangle\langle\psi|$ , we have,  $\text{Tr} [\mathbb{S}_{AA'} \Pi^{\otimes 2} \mathbb{S}_{AA'} \Pi^{\otimes 2}] = \|\rho_A\|_2^4$ , where  $\rho_A \equiv \text{Tr}_B [|\psi\rangle\langle\psi|]$  [39]. That is, the *operator* purity term reduces to the *state* purity squared. Therefore, the connected (and disconnected) BROTOC at zero temperature, for a nondegenerate Hamiltonian probes its groundstate purity.

### 3.4 Long-time limit and eigenstate entanglement

The equilibration value of correlation functions has long been studied as a probe to thermalization and chaos [3, 4]. Although, for finite-dimensional quantum systems, correlation functions typically do not converge to a limit for  $t \rightarrow \infty$ . Instead, after a transient initial period, they oscillate around some equilibrium value [87–90], which can be extracted via long-time averaging (also known as infinite-time averag-

ing), defined as,  $\overline{A(t)} := \lim_{T \rightarrow \infty} \frac{1}{T} \int_0^T A(\tau) d\tau$ . In Refs. [35, 37, 91–93], the equilibration value of the OTOC (or the averaged OTOC) was used to distinguish integrable versus chaotic quantum systems. Here, we discuss how the long-time average of the BROTOC can also reveal the degree of integrability for Hamiltonian quantum systems, and discuss the  $\beta$ -dependence.

A key assumption on the energy spectrum that we will use in this section is the so-called no-resonance condition (NRC) or nondegenerate energy gaps condition [87, 94]. Simply put, both the energy levels and the energy gaps between these levels are nondegenerate. More formally, consider the spectral decomposition of the Hamiltonian,  $H = \sum_{j=1}^d E_j |\phi_j\rangle\langle\phi_j|$ . Then,  $H$  obeys NRC if  $E_l + E_k = E_n + E_m \iff l = n, k = m$  or  $l = m, k = n \quad \forall j, k, l, m$ . The NRC condition is satisfied by *generic* quantum systems and in particular, chaotic quantum systems satisfy such a condition either exactly or to a close approximation. Let us denote by  $\rho_j^\chi := \text{Tr}_\chi [|\phi_j\rangle\langle\phi_j|]$ ,  $\chi = \{A, B\}$  the reduced density matrix corresponding to the  $j$ -th Hamiltonian eigenstate. Moreover, we introduce a Gram matrix corresponding to the inner product between the reduced states,  $R_{jk}^{(\chi)} := \langle \rho_j, \rho_k \rangle$  with  $\chi = \{A, B\}$  and  $\langle \cdot, \cdot \rangle$  the Hilbert-Schmidt inner product. Then, we have the following result.

#### Proposition 4.

$$\overline{G_\beta^{(r)}(t)} = \frac{1}{d\mathcal{Z}(\beta)} \left[ \sum_{j,k=1}^d \exp[-\beta(E_j + E_k)/2] \left( |R_{jk}^A|^2 + |R_{jk}^B|^2 - \delta_{jk} |R_{jk}^A|^2 \right) \right]. \quad (37)$$

This result generalizes to finite-temperature the Proposition 4 obtained in [35] and therefore at  $\beta = 0$ , reduces to the form described there. We can rescale the reduced states as  $\sigma_j^\chi := \exp[-\beta E_j/4] \rho_j^\chi$ , which generates a rescaled Gram matrix  $\tilde{R}_{jk}^{(\chi)} := \langle \sigma_j^\chi, \sigma_k^\chi \rangle = \exp[-\beta(E_j + E_k)/4] \langle \rho_j^\chi, \rho_k^\chi \rangle$ . Therefore, we can rewrite the time-average as,

$$\overline{G_\beta^{(r)}(t)} = \frac{1}{d\mathcal{Z}(\beta)} \sum_{\chi \in \{A, B\}} \left( \left\| \tilde{R}^{(\chi)} \right\|_2^2 - \frac{1}{2} \left\| \tilde{R}_D^{(\chi)} \right\|_2^2 \right), \quad (38)$$

with  $[\tilde{R}_D^{(\chi)}]_{jk} = [\tilde{R}_D^{(\chi)}]_{jk} \delta_{jk}$ .

Similarly, for the disconnected correlator, we have,

$$\begin{aligned} G_\beta^{(d)} &= \frac{1}{d} \left\| \text{Tr}_A [\sqrt{\rho_\beta}] \right\|_2^2 \left\| \text{Tr}_B [\sqrt{\rho_\beta}] \right\|_2^2 \\ &= \frac{1}{d} \left\| \sum_{j=1}^d \frac{\exp[-\beta E_j/2]}{\sqrt{\mathcal{Z}(\beta)}} \rho_j^B \right\|_2^2 \left\| \sum_{k=1}^d \frac{\exp[-\beta E_k/2]}{\sqrt{\mathcal{Z}(\beta)}} \rho_k^A \right\|_2^2 \\ &= \frac{\mathcal{Z}(\beta/2)^4}{d\mathcal{Z}(\beta)^2} \left\| \sum_{j=1}^d p_j(\beta/2) \rho_j^B \right\|_2^2 \left\| \sum_{k=1}^d p_k(\beta/2) \rho_k^A \right\|_2^2, \end{aligned} \quad (39)$$

where  $p_j(\beta) := \exp[-\beta E_j]/\mathcal{Z}(\beta)$  is the Gibbs probability associated to the energy level  $j$  at inverse temperature  $\beta$ .

*Maximally-entangled models.*— **Proposition 4** allows us to connect the equilibration value of the regularized OTOC with the entanglement in the Hamiltonian eigenstates. As a concrete example, we evaluate this equilibration value for a symmetric bipartition, that is,  $d_A = d_B = \sqrt{d}$  and a Hamiltonian whose eigenstates are maximally entangled, that is,  $\{|\phi_k\rangle\}_{k=1}^d$  are maximally entangled across the  $A|B$  partition. We term this Hamiltonian a “maximally entangled Hamiltonian” for brevity. For such a Hamiltonian, we have,  $\rho_k^A = \mathbb{I}/\sqrt{d} = \rho_k^B \quad \forall k$  and therefore,  $R_{k,l}^A = \text{Tr}[\rho_k^A \rho_l^A] = \frac{1}{d} \text{Tr}[I_{\sqrt{d}}] = \frac{1}{\sqrt{d}} = R_{k,l}^B \quad \forall k, l$ . Then, we have,

$$\overline{G_\beta^{(r)}(t)}|_{\text{ME}} = \frac{1}{d^2} \left( \frac{2\mathcal{Z}(\beta/2)^2}{\mathcal{Z}(\beta)} - 1 \right). \quad (40)$$

Notice that this equilibration value is close to the lower bound (for a symmetric bipartition):  $\mathcal{Z}(\beta/2)^2/d^2\mathcal{Z}(\beta) \leq \overline{G_\beta^{(r)}(t)}$ .

Similarly, for the disconnected correlator, one can show that,

$$G_\beta^{(d)}|_{\text{ME}} = \frac{\mathcal{Z}(\beta/2)^4}{d^2\mathcal{Z}(\beta)^2}. \quad (41)$$

Putting everything together, we have, the equilibration value of the BROTOC for a maximally-entangled Hamiltonian is,

$$\overline{N_\beta(t)}|_{\text{ME}} = \frac{1}{d^2} \left( \frac{\mathcal{Z}(\beta/2)^2}{\mathcal{Z}(\beta)} - 1 \right)^2. \quad (42)$$

Notice that at  $\beta = 0$ ,  $\mathcal{Z}(\beta) = \text{Tr}[I] = d = \mathcal{Z}(\beta/2)$ . Therefore, the above evaluates to  $\overline{N_{\beta=0}(t)}|_{\text{ME}} = (1 - \frac{1}{d})^2 = \overline{G}_{\text{ME}}^{\text{NRC}}$  for  $\beta = 0$  as in Ref. [35], which shows that the equilibration value is nearly maximal; which for a symmetric bipartition is equal to  $1 - 1/d$ . For quantum chaotic systems, random matrix theory predicts that the spectral and eigenstate properties of the Hamiltonian resemble those of the Gaussian random matrix ensembles (depending on the universality class) [61, 62], which typically have nearly maximally

entangled eigenstates. Therefore, one can expect the equilibration value to be close to Eq. (42).

We outline here a qualitative argument to understand the decrease of  $G_\beta^{(r)}(t)$  with  $\beta$  as will become evident in the section on Numerical Simulations. In fact, this monotonicity is an *entropic* effect due to the fact that, by increasing  $\beta$ , less and less states contribute to the sum in Proposition 4, the general formula for all Hamiltonians that satisfy NRC. We now make a quantitative argument: let  $\mathbf{p}(\beta/2)$  be a probability vector whose components are  $p_i = \frac{e^{-\beta E_i/2}}{Z(\beta/2)}$ . Then,  $\|\mathbf{p}(\beta/2)\|^2 = Z(\beta)Z(\beta/2)^{-2}$  and we can reexpress the BROTOC as,

$$\overline{G_\beta^{(r)}(t)} = \frac{\langle \mathbf{p}(\beta/2), \hat{C}\mathbf{p}(\beta/2) \rangle}{d\|\mathbf{p}(\beta/2)\|^2}, \quad (43)$$

where  $C_{ij} := |R_{ij}^A|^2 + |R_{ij}^B|^2 - \delta_{ij}|R_{ij}^A|^2$ .

The denominator of Eq. (43) is proportional to the purity of  $\mathbf{p}(\beta/2)$  and it is therefore monotonically increasing with  $\beta$  ( $d^{-1}$  at  $\beta = 0$ , and 1 at  $\beta = \infty$ ). On the other hand, the numerator of Eq. (43) can change from  $O(d_A^{-2})$  at  $\beta = 0$  to  $O(1)$  for local models ( $O(d_A^{-2})$  for non-local ones). This change is always dominated by the purity increase in the denominator. For example in the maximally entangled case ( $d_A = d_B = \sqrt{d}$ ) one has  $C_{ij} = d^{-1}(2 - \delta_{ij})$  and therefore one can rewrite Eq. (40) as

$$\begin{aligned} \overline{G_\beta^{(r)}(t)}|_{\text{ME}} &= \frac{2 - \|\mathbf{p}(\beta/2)\|^2}{d^2\|\mathbf{p}(\beta/2)\|^2} \\ &= \frac{1}{d^2} \frac{1 + S_{\text{lin}}(\beta/2)}{1 - S_{\text{lin}}(\beta/2)}, \end{aligned} \quad (44)$$

where  $S_{\text{lin}}(\beta) := 1 - \|\mathbf{p}(\beta)\|^2$  is the *linear entropy* of  $\rho(\beta)$ . This function is clearly monotonically decreasing with  $\beta$  and shows, once again, that the increase of the time-averaged connected OTOC with temperature is an *entropic* effect.

*Nearly maximally-entangled models.*— We will now show that, if the Hamiltonian eigenstates are highly entangled then it implies a bound on the equilibration value that is close to the maximally entangled case. Recall that a quantum state is called “Page scrambled” [23, 75, 76] if any arbitrary subsystem that consists of up to half of the state’s degrees of freedom are nearly maximally mixed. In the following proposition, we assume Page scrambling of all Hamiltonian eigenstates across a symmetric bipartition  $d_A = d_B = \sqrt{d}$  and show that the equilibration value is close to that of highly entangled models. Let  $\mathcal{P}(|\psi_{AB}\rangle)$  denote the purity of the reduced state of  $|\psi_{AB}\rangle$  across the bipartition  $A|B$  and  $\mathcal{P}_{\min} = \min\{\frac{1}{d_A}, \frac{1}{d_B}\}$  be the minimum purity of a quantum state across the  $A|B$  bipartition. Recall that a pure state  $|\psi_{AB}\rangle$  is maximally entangled across  $A|B \iff \mathcal{P}(|\psi_{AB}\rangle) = \mathcal{P}_{\min}$ . Then, the deviations

from the maximally entangled value are bounded as follows.

**Proposition 5.** *For a symmetric bipartition of the Hilbert space,  $d_A = d_B = \sqrt{d}$  if  $\mathcal{P}(|\psi_{AB}\rangle) - \mathcal{P}_{\min} \leq \epsilon$  holds for all eigenstates, then for systems satisfying NRC, the equilibration value is bounded away from the maximally entangled case as follows,*

$$\left| \overline{G_\beta^{(r)}(t)}|_{\text{ME}} - \overline{G_\beta^{(r)}(t)}|_{\text{NRC}} \right| \leq \frac{\mathcal{Z}(\beta/2)^2}{d\mathcal{Z}(\beta)} \left( \frac{6\epsilon}{\sqrt{d}} + 3\epsilon^2 \right).$$

*Unregularized vs regularized OTOC.*— We highlight a key difference between the bipartite regularized versus unregularized OTOCs. As we will note, for nearly maximally entangled models, the  $G_\beta(t)$  is nearly  $\beta$ -independent, while the  $G_\beta^{(r)}(t)$  shows a clear  $\beta$ -dependence as we have seen above. The proof relies on using an operator Schmidt decomposition for the unitary  $U_t$ , see the Appendix for more details. We obtain that,

$$G_\beta(U) = 1 - F_\beta(U) = 1 - \frac{1}{d_A^2}, \quad (45)$$

and is independent of  $\beta$ . Contrast this, with the equilibration value for nearly maximally entangled Hamiltonians Eq. (42), as computed above. Let us consider Hamiltonians from the Gaussian Unitary Ensemble (GUE) as an example. The eigenstates of these are known to have near maximal entanglement and therefore, we can approximate the  $\overline{N_\beta(t)} \approx \frac{1}{d^2} \left( \frac{\mathcal{Z}(\beta/2)^2}{\mathcal{Z}(\beta)} - 1 \right)^2$ . Moreover, for large- $d$ , the partition function after ensemble averaging can be expressed as [46, 62],  $\langle \mathcal{Z}(\beta) \rangle_{\text{GUE}} = \frac{dI_1(2\beta)}{\beta}$ , where  $I_1(\beta)$  is the modified Bessel function of the first kind. Therefore, the ensemble averaged equilibration value of  $N_\beta(t)$  for the GUE is <sup>1</sup>

$$\overline{\langle N_\beta(t) \rangle}_{\text{GUE}} \approx \left[ \frac{4I_1(\beta)^2}{\beta I_1(2\beta)} - \frac{1}{d} \right]^2. \quad (46)$$

Notice that,  $I_1(2\beta)/\beta = \sum_{n=0}^{\infty} \frac{\beta^{2n}}{(n!)^2(n+1)}$ . Therefore, we can extract from this, both the low- and high-temperature estimates. In Fig. 1 we plot the Bessel function form along with the numerical estimate of the long-time average of the connected BROTOC for the GUE, obtained by averaging (numerically generated) GUE Hamiltonians for  $d = 100$ .

*NRC-product states (NRC-PS).*— We introduce a Hamiltonian model that has a generic spectrum, namely, one that satisfies NRC but with all eigenstates as product states (for example, the computational basis states), that we call “NRC-PS”. The

<sup>1</sup>We have implicitly assumed here that the ensemble averaging and the large- $d$  limits commute, see [22, 95] for a discussion.

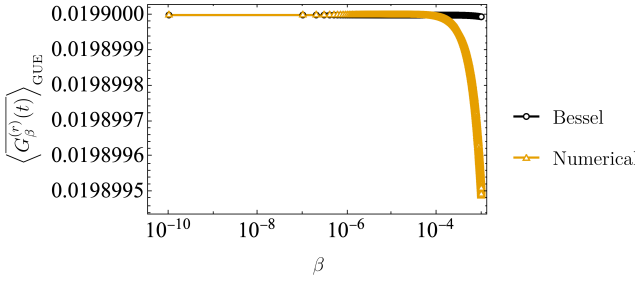


**Figure 1:** A log-log plot of the equilibration value (long-time average) of the  $\bar{G}_\beta^{(r)}(t)$  for the GUE Hamiltonian at  $d = 100$  for  $10^{-10} \leq \beta \leq 10^{-3}$  comparing the numerical estimate to the Bessel function form above.

Hamiltonian can be expressed as,

$$H_{\text{NRC-PS}} := \sum_{j,k=1}^{d_A, d_B} E_{j,k} |\phi_j^{(A)}\rangle\langle\phi_j^{(A)}| \otimes |\phi_k^{(B)}\rangle\langle\phi_k^{(B)}|, \quad (47)$$

where the spectrum  $\{E_{j,k}\}_{j,k}$  satisfies NRC<sup>2</sup>; for example, consider the spectrum of a Hamiltonian from a Gaussian Unitary Ensemble (GUE). The reason to introduce such a model is twofold: first, it allows us to *disentangle* the spectral and eigenstate contributions to the equilibration value  $\bar{G}_\beta^{(r)}(t)$  since, it has the spectrum of a “chaotic” model and the eigenstate properties of a “free” model. Second, as we show now, this model is analytically tractable. The key reason for this is that the NRC-PS model has an extensive number of conserved quantities,  $d = 2^L$  of them in fact. A local operator of the form,  $A_j = |\phi_j^A\rangle\langle\phi_j^A| \otimes \mathbb{I}$  commutes with the Hamiltonian above,  $[H, A_j] = 0 \ \forall j \in \{1, 2, \dots, d_A\}$ . Similarly, operators of the form,  $B_k = \mathbb{I} \otimes |\phi_k^B\rangle\langle\phi_k^B|$  also commute with the Hamiltonian,  $[H, B_k] = 0 \ \forall k \in \{1, 2, \dots, d_B\}$ . Therefore, the Hamiltonian has  $d = d_A d_B$  number of local conserved quantities. In this sense, this is an integrable model, notice however, that its spectrum is intentionally chosen to satisfy NRC.

The presence of conserved quantities enable an exact calculation for the equilibration value of the BRO-TOC in this model. A detailed proof of this can be found in the Appendix.

$$\overline{G_\beta^{(r)}(t)}|_{\text{NRC-PS}} = \frac{1}{d} \left( \frac{\|\mathbf{p}^A(\beta/2)\|^2 + \|\mathbf{p}^B(\beta/2)\|^2}{\|\mathbf{p}(\beta/2)\|^2} - 1 \right) \quad (48)$$

<sup>2</sup>Note that any Hamiltonian that satisfies NRC cannot be noninteracting, i.e., cannot be of the form  $H = H_A \otimes \mathbb{I}_B + \mathbb{I}_A \otimes H_B$  since such a Hamiltonian would, by construction, violate NRC. As an example, consider product eigenstates of the form,  $\{|\phi_j^{(A)}\rangle \otimes |\chi_k^{(B)}\rangle\}_{j,k}$  then it is easy to find pairs of eigenstates for which the energy gaps are equal [94]. However, the converse is not true, namely, there exist interacting Hamiltonians, i.e., of the form  $H \neq H_A \otimes \mathbb{I}_B + \mathbb{I}_A \otimes H_B$  that have product eigenstates.

where the probability vector  $\mathbf{p}(\beta)$  is as in the above and  $\mathbf{p}^{A/B}(\beta)$  are its marginals e.g.,  $\mathbf{p}_j^A(\beta) = \sum_{k=1}^{d_B} \mathbf{p}_{jk}(\beta) = \frac{1}{Z(\beta)} \sum_{k=1}^{d_B} e^{-\beta E_{jk}}$ .

From this Equation one finds immediately  $\overline{G_{\beta=0}^{(r)}(t)}|_{\text{NRC-PS}} = 1/d_A + 1/d_B - 1/d > 1/d$  at infinite temperature and,  $\overline{G_{\beta=\infty}^{(r)}(t)}|_{\text{NRC-PS}} = 1/d$  at zero temperature. For a symmetric bipartition  $d_A = d_B = \sqrt{d}$ , the former simplifies to  $2/\sqrt{d} - 1/d = O(1/\sqrt{d})$ . And, as we will see in the next section, the numerical data obtained from finite-size scaling in Tables 1 and A1 is consistent with this as  $\overline{G_\beta^{(r)}(t)} \approx \frac{2}{\sqrt{d}}$ .

## 4 Numerical simulations

In this section we study numerically various dynamical features of the BRO-TOC. In particular, we vary the *degree* of integrability of Hamiltonian systems and quantify its effect on the equilibration value  $\overline{G_\beta^{(r)}(t)}$ . At  $\beta = 0$ , this is equal to one minus the operator entanglement of the dynamical unitary, whose equilibration value was used to distinguish various integrable and chaotic models in Ref. [35], see also Refs. [53, 91, 92, 96] for distinguishing integrable and chaotic models via time-averages of the OTOC or operator entanglement. We also refer the reader to Ref. [97], where bounds on decay of OTOCs in time were obtained using the scaling of the time-averaged OTOC. Here, we perform more extensive numerical studies, consider more generally the  $\beta$ -dependence of this quantity, and focus on the following Hamiltonian models of interest:

1. **Integrable model:** The transverse-field Ising model (TFIM) with the Hamiltonian,  $H_{\text{TFIM}} = -\sum_{j=1}^{L-1} \sigma_j^z \sigma_{j+1}^z - g \sum_{j=1}^L \sigma_j^x - h \sum_{j=1}^L \sigma_j^z$ , as a paradigmatic quantum spin-chain model. Here, the  $\sigma_j^\alpha, \alpha \in \{x, y, z\}$  are the Pauli matrices. For the TFIM,  $g, h$  denotes the strength of the transverse field and the local field, respectively. The TFIM Hamiltonian is integrable for either  $h = 0$  or  $g = 0$  and nonintegrable when both  $g, h$  are nonzero. We consider as the integrable point,  $g = 1, h = 0$  and the nonintegrable point  $g = -1.05, h = 0.5$ . At the integrable point, this model can be mapped onto free fermions via the Jordan-Wigner transformation and is “highly integrable” in this sense. At the nonintegrable point, the model is quantum chaotic, in the sense of random matrix spectral statistics [98, 99] and volume-law entanglement of eigenstates [100].

2. **Localized models:** We study Anderson and

many-body localization (MBL) with the Hamiltonian,  $H_{\text{MBL}} = -\sum_{j=1}^{L-1} \sigma_j^z \sigma_{j+1}^z - \sum_{j=1}^L g_j \sigma_j^x - h \sum_{j=1}^L \sigma_j^z$ , where we draw from the uniform distribution, each  $g_j \in [-\eta, \eta]$ . In the absence of the longitudinal field, i.e.,  $h = 0$ , and for nonzero disorder, this (disordered) free fermion model is Anderson localized. In the presence of the longitudinal field, the fermions are interacting and at sufficiently strong disorder, the model is many-body localized (MBL). As is well-known, MBL escapes thermalization by emergent integrability [3, 101]. We refer the reader to Ref. [102] for a discussion of the long-time values of the *unregularized* OTOC in localized phases. In our numerical simulations, we focus on  $\eta = 10$  for the disorder strength and  $h = 0.1$  for the MBL case. We average each instance of the disordered model over  $\lfloor 200/L \rfloor$  independent realizations. In each case, the error bars are too small to plot alongside the data points.

3. NRC-product states (NRC-PS): As introduced before this model allows us to separate the *spectral* and *eigenstate* contributions to the BRO-TOC's equilibration value. We choose a “chaotic” spectrum (in the sense that it corresponds to a GUE Hamiltonian and hence is an instance of a model that obeys Wigner-Dyson statistics), while having the eigenstates of a *noninteracting* model, that is, simple product states. To study the NRC-PS model numerically, we generate a random matrix from the Gaussian Unitary Ensemble (GUE) and use its spectrum, while keeping product eigenstates. We average this numerically over  $\lfloor 200/L \rfloor$  independent realizations. This yields numerical results consistent with the analytical expression obtained from Eq. (48).
4. Random matrices: As a benchmark for a “maximally chaotic” model, we consider Hamiltonians drawn from the GUE. For Hamiltonian systems, the seminal works of Berry and Tabor [103] and that of Bohigas, Giannoni, and Schmit [104] establishes that Poisson level-statistics is a characteristic feature of integrable, while for thermalizing systems, Wigner-Dyson statistics are the norm [2, 101]. Furthermore, the eigenstates of GUE are nearly maximally entangled and will provide an analytically tractable example of a highly chaotic model. For our numerical simulations, we generate random matrices and average over  $\lfloor 200/L \rfloor$  independent realizations. The error bars are too small to plot alongside the data points in this case as well. The “ME” in the plots corresponds to a maximally entangled model for which we use the

analytical expressions from Eq. (40). For this we generate the spectrum from the GUE and average over  $\lfloor 200/L \rfloor$  independent realizations.

Throughout this section, to evaluate the time-averages  $\overline{G_\beta^{(r)}(t)}$  numerically, we use two different methods. First, for the Anderson and TFIM integrable model, since it does not satisfy NRC (the Hamiltonian has symmetries), we perform exact time evolution. We do this for a time interval of  $t \in [10, 10^3]$  with a  $10^6$  time steps in between. This is fixed for all the system sizes  $L$  and inverse temperatures  $\beta$ . All models except these two satisfy NRC (also verified numerically) and so we compute  $\overline{G_\beta^{(r)}(t)}$  using the analytical expression in Proposition 4. To do this, we perform exact diagonalization of the full Hamiltonian for this and compute the reduced states. At large  $\beta$ , it is easy to show that one only needs the ground state along with a few excited states to estimate the time-average in Proposition 4. Therefore, for  $L = 13, 14$  and  $\beta = 1$ , we only extract the lowest 20 Hamiltonian eigenstates.

The first numerical result focusses on  $L = 6$  qubits and we study the variation of  $\overline{G_\beta^{(r)}(t)}$  as a function of  $\beta$ . In Fig. 2, we notice the following *universal features* of  $\overline{G_\beta^{(r)}(t)}$  as a function of  $\beta$ : the equilibration value is very slowly decaying as  $\beta$  varies from zero to  $O(1)$ . Around  $\beta = O(1)$ , the equilibration value quickly decays to the asymptotic value. Using, Proposition 3, we note that the asymptotic value  $\beta \rightarrow \infty$  is proportional to the operator purity for the ground state projector. With these universal features at hand, we systematically study the equilibration value  $\overline{G_\beta^{(r)}(t)}$  for three representative choices of  $\beta$ :  $\beta = 0, \beta = 1$  and  $\beta \rightarrow \infty$ . We numerically study their scaling as a function of the system size for a symmetric bipartition of the lattice,  $\lfloor L/2 \rfloor : \lceil L/2 \rceil$ . For the case where  $L$  is not even, the numerical results are very similar for either choice of bipartition,  $\lfloor L/2 \rfloor : \lceil L/2 \rceil$  or  $\lceil L/2 \rceil : \lfloor L/2 \rfloor$ , and therefore, we choose the former throughout. We also label as “logplot” a plot with logarithmic scale on the  $y$ -axis and “loglogplot” those with logarithmic scale on both  $x$ - and  $y$ -axes.

The results for  $\beta = 0$  are discussed in Fig. 3. We notice that the scaling w.r.t. the system size is effectively divided into two classes: the quantum chaotic models, namely, the nonintegrable TFIM and the GUE. And, the second class is all the others, namely, the free fermions, the Anderson and MBL, and the NRC-PS. These two classes are primarily distinguished by their eigenstate entanglement, namely, the scaling of the entanglement across the entire spectrum. This, perhaps, comes as no surprise since the infinite-temperature OTOC by construction probes the entanglement across all eigenstates.

At  $\beta = 1$ , from Fig. 4, we notice that the MBL and quantum chaotic models have merged, while having a distinct scaling from the other integrable models and the GUE. Recall that at  $\beta = 0$ , Theorem 6 of Ref. [35] establishes a hierarchy between the equilibration values of various estimates for the equilibration value. However, for the regularized OTOC, this result does not necessarily hold away from the  $\beta = 0$  case since now we have extra  $H$ -dependent terms in the NRC estimate; see [Proposition 3](#).

And finally, the scaling for  $\beta = \infty$  can be understood using [Proposition 3](#). For the nondegenerate Hamiltonians, this simply probes the ground state entanglement. We notice that all curves coalesce into two groups, one for the integrable/localized models and the second for the GUE and ME models, respectively. While these models vary in their degree of integrability, their ground states (apart from the GUE/ME) all follow an area law [100] and hence obey a different decay rate with  $L$  from the GUE. Note that the GUE ground state is a Haar random state and therefore, should scale as  $\overline{G_{\beta \rightarrow \infty}^{(r)}(t)} \sim \frac{1}{d^2}$ , which is consistent with the finite-size scaling results.

Model	$\beta = 0$	$\beta = 1$	$\beta = \infty$
TFIM integrable	0.507672	0.687979	1.01858
NRC-PS	0.495827	0.7218	1.00
Anderson	0.557617	0.655576	1.00
MBL	0.491745	0.883465	1.00075
TFIM chaotic	1.00781	0.884371	0.999999
GUE	0.999992	1.76251	2.00016

**Table 1:** The decay rate  $\gamma$  for various Hamiltonian models at  $\beta = 0, 1, \infty$ , with respect to the Ansatz  $\overline{G_{\beta}^{(r)}(t)} = \alpha d^{-\gamma}$ . The prefactor  $\alpha$  is *nonuniversal*, the details of which can be found in the Appendix.

*Finite-size scaling.*— To quantitatively understand the numerical results, we perform finite-size scaling analysis for each choice of  $\beta$ . Let us start with the infinite-temperature case ( $\beta = 0$ ). We consider an Ansatz of the form,

$$\overline{G_{\beta}^{(r)}(t)} = \alpha d^{-\gamma} + \overline{G_{\beta}^{(r)}(t)}_{\infty}, \quad (49)$$

where  $d$  is the Hilbert space dimension and  $\overline{G_{\beta}^{(r)}(t)}_{\infty}$  is the asymptotic value, i.e., as  $d \rightarrow \infty$ . From several analytical and numerical results, we know that  $\overline{G_{\beta}^{(r)}(t)}_{\infty} = 0$ . That is, the BROTOC decays for all models, free, integrable, or chaotic. Therefore, we reduce the Ansatz to

$$\overline{G_{\beta}^{(r)}(t)} = \alpha d^{-\gamma}. \quad (50)$$

As a result, we have,  $\log_2(\overline{G_{\beta}^{(r)}(t)}) = \log_2(\alpha) + (-\gamma) L$  where  $2^L = d$ . The numerical results naturally manifest this Ansatz as is evident from the nearly linear figures. Therefore, performing a linear fit to the  $\log_2(\overline{G_{\beta}^{(r)}(t)})$  versus  $L$  plots yields the decay rates corresponding to various models. We focus on the last 5 data points to obtain the fit parameters, see the Appendix for more details.

The finite-size scaling results are summarized in [Table 1](#). The decay rates are *universal* at  $\beta = 0$  with  $\gamma \approx 0.5$  for the integrable models and  $\gamma \approx 1$  for the chaotic models. Around  $\beta = O(1)$ , this universality begins to breakdown and at large  $\beta$ , the equilibration value  $\overline{G_{\beta}^{(r)}(t)}$  only differentiates local models from the nonlocal GUE model.

From the analytical results about NRC-PS and GUE, we know that at  $\beta = 0$ , the  $\gamma_{\text{NRC-PS}} = \frac{1}{2}\gamma_{\text{GUE}}$ . And, from the finite-size scaling results, we obtain,  $\gamma_{\text{NRC-PS}}/\gamma_{\text{GUE}} \approx 0.495831$ . At  $\beta \rightarrow \infty$ , using [Proposition 3](#), for both NRC-PS and GUE, the equilibration value is determined by the ground state purity. Therefore, for NRC-PS, it scales as  $\frac{1}{d}$  and for GUE it scales as  $\frac{1}{d^2}$  since GUE ground states are Haar-random states, their purity is near minimum, with  $O(\frac{1}{d})$  corrections, which is also consistent with the finite-size scaling results. Therefore, the ratio of the rates in this case is also  $\frac{1}{2}$ . And finally, from the numerical values listed in [Table 1](#), we see that the ratio is  $\approx \frac{1}{2}$  at  $\beta = 1$  as well.

## 5 Conclusions

In this work we introduce the bipartite regularized OTOC that allows us to obtain a wealth of analytical and numerical results to aid our understanding of regularized OTOCs for local quantum systems. The infinite-temperature OTOC has several operational interpretations in terms of operator entanglement, entropy production, and others. [Proposition 1](#) estab-

lished the connected component of the BROTOC as probing the operator purity of a quantum operation. We then showed that the quantum operation  $\mathcal{U}_{\beta,t}$  is intimately related to the two-point spectral form factor and globally averaged regularized OTOCs are connected to the four-point spectral form factor, respectively. Moreover, the connected BROTOC probes the purity of the associated thermofield double state.

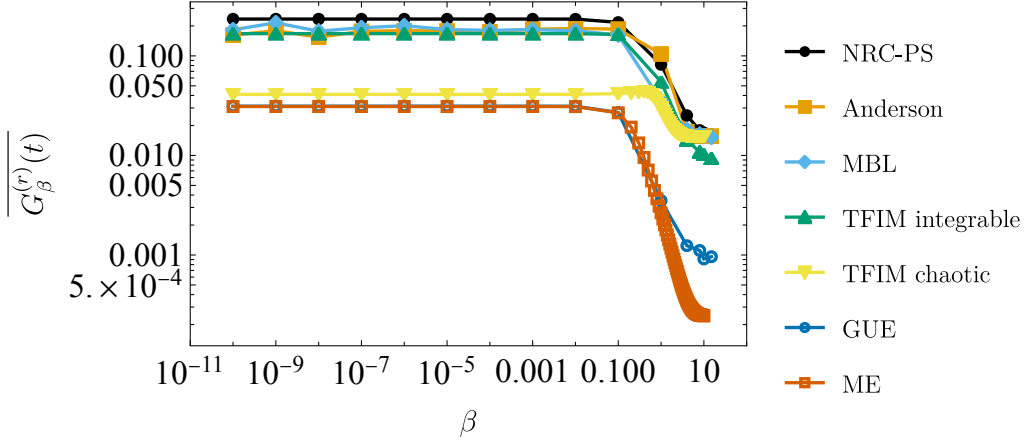


**Figure 2:** A log-log plot of the equilibration value (long-time average) of the  $\overline{G}_\beta^{(r)}(t)$  for various Hamiltonian models at  $L = 6$  as a function of the inverse temperature  $\beta$  across a symmetric bipartition  $L/2 : L/2$ . We use exact time evolution for the integrable TFIM and Anderson since they do not satisfy NRC. For Anderson, MBL, and GUE, we perform exact diagonalization of the full Hamiltonian and use the analytical expression in [Proposition 4](#). For NRC-PS and ME (maximally entangled model), we use the analytical expressions in [Eq. \(40\)](#) and [Eq. \(48\)](#).

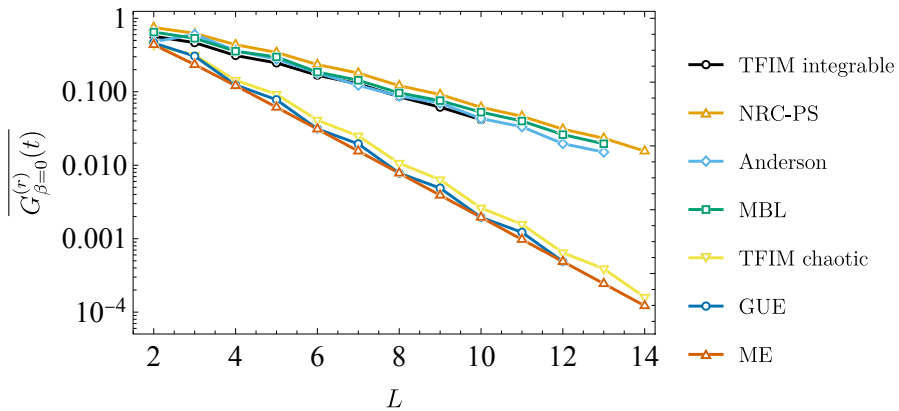


**Figure 3:** A logplot of the equilibration value (long-time average) of the  $\overline{G}_\beta^{(r)}(t)$  for various Hamiltonian models as a function of the system size  $L$  at  $\beta = 0$  across a symmetric bipartition  $[L/2] : [L/2]$ . We use exact time evolution for the integrable TFIM and Anderson since they do not satisfy NRC. For Anderson, MBL, and GUE, we perform exact diagonalization of the full Hamiltonian and use the analytical expression in [Proposition 4](#). For NRC-PS and ME (maximally entangled model), we use the analytical expressions in [Eq. \(40\)](#) and [Eq. \(48\)](#).

Moving away from the infinite-temperature assumption, we investigate the zero-temperature case, where, in [Proposition 3](#), we showed that, in this limit, both the disconnected and connected components of the BROTOC probe the groundstate entanglement for nondegenerate Hamiltonians. This allows us to think of them as probes to quantum phase transitions in the system.

In [Propositions 4 and 5](#), we study the equilibration value of the BROTOC and how it connects to *eigenstate entanglement*. In fact, we show that if there is sufficient entanglement in all eigenstates across the spectrum, then the equilibration value must be nearly maximal. We also obtain analytical closed-form expressions for the equilibration value of nearly maximally-entangled Hamiltonians and contrast the

$\beta$ -dependence in the unregularized versus the regularized case.

Finally, we perform numerical simulations on various integrable and chaotic Hamiltonian models to study the equilibration value of the connected component of the BROTOC. Using a mix of finite-size scaling and analytical estimates, we contrast the decay rates of the BROTOC for various models. While at  $\beta = 0$ , the decay rate is universal and distinguishes integrable, chaotic, and random matrix evolutions; as we reach  $\beta = O(1)$ , this universality begins to break down. And, in fact, at  $\beta \rightarrow \infty$ , the equilibration value only distinguishes local models from the GUE, and is therefore no longer a reliable signature of chaotic-vs-integrable dynamics. An interesting future work would be to contrast various choices of regular-

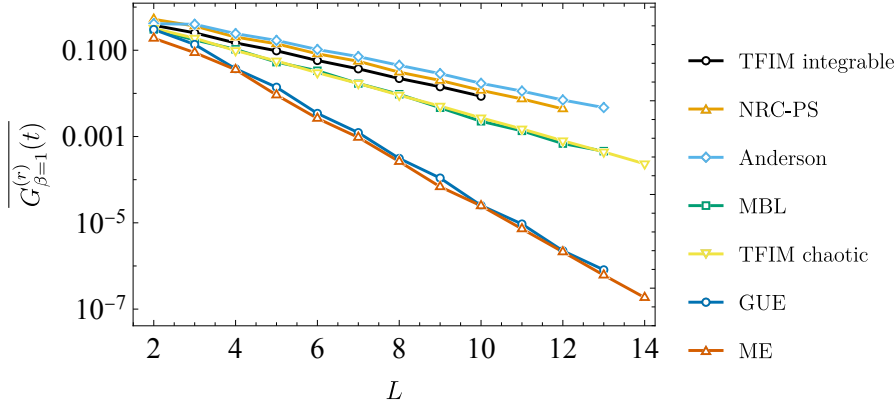


**Figure 4:** A logplot of the equilibration value (long-time average) of the  $\bar{G}_\beta^{(r)}(t)$  for various Hamiltonian models as a function of the system size  $L$  at  $\beta = 1$  across a symmetric bipartition  $[L/2] : [L/2]$ . We use exact time evolution for the integrable TFIM and Anderson since they do not satisfy NRC. For Anderson, MBL, and GUE, we perform exact diagonalization of the full Hamiltonian and use the analytical expression in [Proposition 4](#). For NRC-PS and ME (maximally entangled model), we use the analytical expressions in Eq. [\(40\)](#) and Eq. [\(48\)](#).

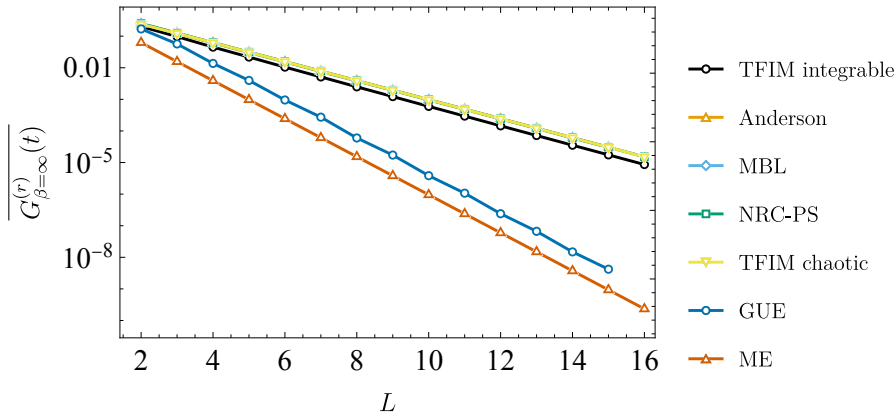


**Figure 5:** A logplot of the equilibration value (long-time average) of the  $\bar{G}_\beta^{(r)}(t)$  for various Hamiltonian models as a function of the system size  $L$  at  $\beta = \infty$  across a symmetric bipartition  $[L/2] : [L/2]$ . The various data points have coalesced into two curves, first consisting of all the integrable models, whose ground state follow area-law entanglement. And second, for the GUE and ME (maximally entangled model), whose ground states follow volume-law entanglement. Using [Proposition 3](#), we simply compute the ground state projector for various models to compute this numerically.

izations and their ability to distinguish chaotic and integrable dynamics.

## 6 Acknowledgments

N.A. would like to thank G. Styliaris for many insightful discussions. The authors acknowledge the Center for Advanced Research Computing (CARC) at the University of Southern California for providing computing resources that have contributed to the research results reported within this publication. URL: <https://carc.usc.edu>. The authors acknowledge partial support from the NSF award PHY-1819189. This research was (partially) sponsored by the Army Research Office and was accomplished under Grant Number W911NF-20-1-0075. The views and conclusions contained in this document are those of the au-

thors and should not be interpreted as representing the official policies, either expressed or implied, of the Army Research Office or the U.S. Government. The U.S. Government is authorized to reproduce and distribute reprints for Government purposes notwithstanding any copyright notation herein.

## References

- [1] M. Srednicki, *Physical Review E* **50**, 888 (1994).
- [2] M. Rigol, V. Dunjko, and M. Olshanii, *Nature* **452**, 854 (2008).
- [3] L. D'Alessio, Y. Kafri, A. Polkovnikov, and M. Rigol, *Advances in Physics* **65**, 239 (2016).
- [4] F. Borgonovi, F. Izrailev, L. Santos, and V. Zelevinsky, *Physics Reports* **626**, 1 (2016).
- [5] C. W. von Keyserlingk, T. Rakovszky, F. Poll-

mann, and S. L. Sondhi, *Phys. Rev. X* **8**, 021013 (2018).

[6] A. Nahum, S. Vijay, and J. Haah, *Phys. Rev. X* **8**, 021014 (2018).

[7] T. Rakovszky, F. Pollmann, and C. W. von Keyserlingk, *Phys. Rev. X* **8**, 031058 (2018).

[8] V. Khemani, A. Vishwanath, and D. A. Huse, *Phys. Rev. X* **8**, 031057 (2018).

[9] S. Gopalakrishnan, D. A. Huse, V. Khemani, and R. Vasseur, *Phys. Rev. B* **98**, 220303 (2018).

[10] A. Chan, A. De Luca, and J. T. Chalker, *Phys. Rev. X* **8**, 041019 (2018).

[11] D. E. Parker, X. Cao, A. Avdoshkin, T. Scaffidi, and E. Altman, *Physical Review X* **9**, 041017 (2019).

[12] C. Murthy and M. Srednicki, *Physical Review Letters* **123**, 230606 (2019).

[13] J. Maldacena, S. H. Shenker, and D. Stanford, *Journal of High Energy Physics* **2016**, 1 (2016).

[14] T. Xu, T. Scaffidi, and X. Cao, *Phys. Rev. Lett.* **124**, 140602 (2020).

[15] B. Swingle, *Nature Physics* **14**, 988 (2018).

[16] S. Xu and B. Swingle, *arXiv:2202.07060* (2022).

[17] I. A. Larkin and Y. N. Ovchinnikov, *Journal of Experimental and Theoretical Physics* **28**, 2262 (1969).

[18] A. Kitaev, “A simple model of quantum holography (part 1),” <http://online.kitp.ucsb.edu/online/entangled15/kitaev/> (2015).

[19] E. H. Lieb and D. W. Robinson, in *Statistical mechanics* (Springer, 1972) pp. 425–431.

[20] M. B. Hastings and T. Koma, *Communications in Mathematical Physics* **265**, 781 (2006).

[21] S. Bravyi, M. B. Hastings, and F. Verstraete, *Physical Review Letters* **97**, 050401 (2006).

[22] J. Cotler, N. Hunter-Jones, J. Liu, and B. Yoshida, *J. High Energ. Phys.* **2017**, 48 (2017).

[23] P. Hosur, X.-L. Qi, D. A. Roberts, and B. Yoshida, *Journal of High Energy Physics* **2016**, 1 (2016).

[24] X. Mi, P. Roushan, C. Quintana, S. Mandrà, J. Marshall, C. Neill, F. Arute, K. Arya, J. Atalaya, R. Babbush, *et al.*, *Science* **374**, 1479 (2021).

[25] J. Braumüller, A. H. Karamlou, Y. Yanay, B. Kannan, D. Kim, M. Kjaergaard, A. Melville, B. M. Niedzielski, Y. Sung, A. Vepsäläinen, *et al.*, *Nature Physics* **18**, 172 (2022).

[26] K. X. Wei, C. Ramanathan, and P. Cappellaro, *Phys. Rev. Lett.* **120**, 070501 (2018).

[27] J. Li, R. Fan, H. Wang, B. Ye, B. Zeng, H. Zhai, X. Peng, and J. Du, *Physical Review X* **7**, 031011 (2017).

[28] X. Nie, Z. Zhang, X. Zhao, T. Xin, D. Lu, and J. Li, *arXiv:1903.12237* (2019).

[29] X. Nie, B.-B. Wei, X. Chen, Z. Zhang, X. Zhao, C. Qiu, Y. Tian, Y. Ji, T. Xin, D. Lu, and J. Li, *Phys. Rev. Lett.* **124**, 250601 (2020).

[30] M. Gärttner, J. G. Bohnet, A. Safavi-Naini, M. L. Wall, J. J. Bollinger, and A. M. Rey, *Nature Physics* **13**, 781 (2017).

[31] M. K. Joshi, A. Elben, B. Vermersch, T. Brydges, C. Maier, P. Zoller, R. Blatt, and C. F. Roos, *Phys. Rev. Lett.* **124**, 240505 (2020).

[32] E. J. Meier, J. Ang’ong’aa, F. A. An, and B. Gadway, *Phys. Rev. A* **100**, 013623 (2019).

[33] B. Chen, X. Hou, F. Zhou, P. Qian, H. Shen, and N. Xu, *Applied Physics Letters* **116**, 194002 (2020).

[34] B. Yan, L. Cincio, and W. H. Zurek, *Phys. Rev. Lett.* **124**, 160603 (2020).

[35] G. Styliaris, N. Anand, and P. Zanardi, *Physical Review Letters* **126**, 030601 (2021).

[36] P. Zanardi and N. Anand, *Physical Review A* **103**, 062214 (2021).

[37] N. Anand, G. Styliaris, M. Kumari, and P. Zanardi, *Phys. Rev. Research* **3**, 023214 (2021).

[38] N. Yunger Halpern, A. Bartolotta, and J. Pollock, *Commun Phys* **2**, 92 (2019).

[39] P. Zanardi, *Phys. Rev. A* **63**, 040304 (2001).

[40] X. Wang and P. Zanardi, *Phys. Rev. A* **66**, 044303 (2002).

[41] P. Zanardi, C. Zalka, and L. Faoro, *Phys. Rev. A* **62**, 030301 (2000).

[42] A. Touil and S. Deffner, *PRX Quantum* **2**, 010306 (2021).

[43] J. Watrous, *The Theory of Quantum Information*, 1st ed. (Cambridge University Press, 2018).

[44] N. Tsuji, T. Shitara, and M. Ueda, *Physical Review E* **98**, 012216 (2018).

[45] L. Foini and J. Kurchan, *Physical Review E* **99**, 042139 (2019).

[46] S. Vijay and A. Vishwanath, *arXiv:1803.08483* (2018).

[47] S. Sahu and B. Swingle, *Physical Review B* **102**, 184303 (2020).

[48] Y. Liao and V. Galitski, *Phys. Rev. B* **98**, 205124 (2018).

[49] M. A. Nielsen and I. L. Chuang, *Quantum Computation and Quantum Information*, 10th ed. (Cambridge University Press, Cambridge ; New York, 2010).

[50] M. B. Plenio and S. Virmani, *arXiv:quant-ph/0504163* (2005).

[51] C. Lupo, P. Aniello, and A. Scardicchio, *Journal of Physics A: Mathematical and Theoretical* **41**, 415301 (2008).

[52] P. Aniello and C. Lupo, *Open Systems and Information Dynamics* **16**, 127–143 (2009).

[53] T. Zhou and D. J. Luitz, *Phys. Rev. B* **95**, 094206 (2017).

[54] I. Kukuljan, S. Grozdanov, and T. Prosen, *Phys. Rev. B* **96**, 060301 (2017).

[55] C.-J. Lin and O. I. Motrunich, *Phys. Rev. B* **97**, 144304 (2018).

[56] X. Chen and T. Zhou, *Phys. Rev. B* **100**, 064305 (2019).

[57] V. Khemani, D. A. Huse, and A. Nahum, *Phys. Rev. B* **98**, 144304 (2018).

[58] Y. Chen, arXiv:1608.02765 (2016).

[59] A. Avdoshkin and A. Dymarsky, *Phys. Rev. Research* **2**, 043234 (2020).

[60] F. Haake, *Quantum Signatures of Chaos*, 3rd ed., Springer Series in Synergetics No. 54 (Springer, Berlin ; New York, 2010).

[61] T. Guhr, A. Müller-Groeling, and H. A. Weidenmüller, *Physics Reports* **299**, 189 (1998).

[62] M. L. Mehta, *Random Matrices*, 3rd ed., Pure and Applied Mathematics Series No. 142 (Elsevier, Amsterdam, 2004).

[63] M. V. Berry, *Proc. R. Soc. Lond. A* **400**, 229 (1985).

[64] Y. Takahashi and H. Umezawa, *International Journal of Modern Physics B* **10**, 1755 (1996).

[65] E. Dyer and G. Gur-Ari, *J. High Energ. Phys.* **2017**, 75 (2017).

[66] A. del Campo, J. Molina-Vilaplana, and J. Sonner, *Physical Review D* **95**, 126008 (2017).

[67] K. Papadodimas and S. Raju, *Phys. Rev. Lett.* **115**, 211601 (2015).

[68] J. Wu and T. H. Hsieh, *Phys. Rev. Lett.* **123**, 220502 (2019).

[69] J. Martyn and B. Swingle, *Phys. Rev. A* **100**, 032107 (2019).

[70] D. Zhu, S. Johri, N. M. Linke, K. A. Landsman, C. Huerta Alderete, N. H. Nguyen, A. Y. Matsuura, T. H. Hsieh, and C. Monroe, *Proc. Natl. Acad. Sci. U.S.A.* **117**, 25402 (2020).

[71] W. Cottrell, B. Freivogel, D. M. Hofman, and S. F. Lokhande, *J. High Energ. Phys.* **2019**, 58 (2019).

[72] E. Lantagne-Hurtubise, S. Plugge, O. Can, and M. Franz, *Phys. Rev. Research* **2**, 013254 (2020).

[73] J. Cotler, N. Hunter-Jones, J. Liu, and B. Yoshida, *Journal of High Energy Physics* **2017** (2017), 10.1007/JHEP11(2017)048.

[74] M. M. Wilde, *From Classical to Quantum Shannon Theory*, cambridge university press ed. (2016).

[75] Y. Sekino and L. Susskind, *Journal of High Energy Physics* **2008**, 065–065 (2008).

[76] N. Lashkari, D. Stanford, M. Hastings, T. Osborne, and P. Hayden, *J. High Energ. Phys.* **2013**, 22 (2013).

[77] L. Sá, P. Ribeiro, and T. Prosen, *Journal of Physics A: Mathematical and Theoretical* **53**, 305303 (2020).

[78] S. Denisov, T. Laptyeva, W. Tarnowski, D. Chruściński, and K. Życzkowski, *Phys. Rev. Lett.* **123**, 140403 (2019).

[79] T. Can, *Journal of Physics A: Mathematical and Theoretical* **52**, 485302 (2019).

[80] T. Can, V. Oganesyan, D. Orgad, and S. Gopalakrishnan, *Phys. Rev. Lett.* **123**, 234103 (2019).

[81] R. Grobe, F. Haake, and H.-J. Sommers, *Phys. Rev. Lett.* **61**, 1899 (1988).

[82] G. Akemann, M. Kieburg, A. Mielke, and T. c. v. Prosen, *Phys. Rev. Lett.* **123**, 254101 (2019).

[83] L. Sá, P. Ribeiro, and T. Prosen, *Physical Review X* **10**, 021019 (2020).

[84] W. H. Zurek and J. P. Paz, *Physical Review Letters* **72**, 2508 (1994).

[85] S. Sachdev, *Quantum Phase Transitions*, second edition ed. (Cambridge University Press, Cambridge ; New York, 2011).

[86] M. Heyl, F. Pollmann, and B. Dóra, *Phys. Rev. Lett.* **121**, 016801 (2018).

[87] P. Reimann, *Phys. Rev. Lett.* **101**, 190403 (2008).

[88] N. Linden, S. Popescu, A. J. Short, and A. Winter, *Phys. Rev. E* **79**, 061103 (2009).

[89] L. Campos Venuti, N. T. Jacobson, S. Santra, and P. Zanardi, *Phys. Rev. Lett.* **107**, 010403 (2011).

[90] A. M. Alhambra, J. Riddell, and L. P. García-Pintos, *Phys. Rev. Lett.* **124**, 110605 (2020).

[91] I. García-Mata, M. Saraceno, R. A. Jalabert, A. J. Roncaglia, and D. A. Wisniacki, *Phys. Rev. Lett.* **121**, 210601 (2018).

[92] E. M. Fortes, I. García-Mata, R. A. Jalabert, and D. A. Wisniacki, *Phys. Rev. E* **100**, 042201 (2019).

[93] Y. Huang, F. G. S. L. Brandão, and Y.-L. Zhang, *Phys. Rev. Lett.* **123**, 010601 (2019).

[94] A. J. Short, *New Journal of Physics* **13**, 053009 (2011).

[95] Z. Xu, A. Chenu, T. Prosen, and A. del Campo, *Phys. Rev. B* **103**, 064309 (2021).

[96] E. M. Fortes, I. García-Mata, R. A. Jalabert, and D. A. Wisniacki, *EPL (Europhysics Letters)* **130**, 60001 (2020).

[97] V. Balachandran, G. Benenti, G. Casati, and D. Poletti, *Phys. Rev. B* **104**, 104306 (2021).

[98] M. C. Bañuls, J. I. Cirac, and M. B. Hastings, *Phys. Rev. Lett.* **106**, 050405 (2011).

[99] H. Kim and D. A. Huse, *Phys. Rev. Lett.* **111**, 127205 (2013).

[100] M. M. Wolf, F. Verstraete, M. B. Hastings, and J. I. Cirac, *Phys. Rev. Lett.* **100**, 070502 (2008).

[101] R. Nandkishore and D. A. Huse, *Annual Review of Condensed Matter Physics* **6**, 15 (2015).

[102] X. Chen, T. Zhou, D. A. Huse, and E. Fradkin, *Annalen der Physik* **529**, 1600332 (2017).

[103] M. V. Berry and M. Tabor, *Proc. R. Soc. Lond. A* **356**, 375 (1977).

[104] O. Bohigas, M. J. Giannoni, and C. Schmit, *Physical Review Letters* **52**, 1 (1984).

[105] F. A. Pollock, C. Rodríguez-Rosario, T. Frauenheim, M. Paternostro, and K. Modi, *Phys. Rev. A* **97**, 012127 (2018).

[106] F. A. Pollock, C. Rodríguez-Rosario, T. Frauenheim, M. Paternostro, and K. Modi, *Phys. Rev. Lett.* **120**, 040405 (2018).

## Appendices

### Proof of Proposition 1

**Proposition 1.** *The regularized bipartite OTOC at finite temperature is*

$$\begin{aligned} N_\beta(t) &= \frac{1}{d} \mathcal{P}_A(\sqrt{\rho_\beta}) \mathcal{P}_B(\sqrt{\rho_\beta}) \\ &\quad - \frac{1}{d\mathcal{Z}_\beta} \text{Tr} \left[ \mathbb{S}_{AA'} \mathcal{U}_{\beta,t}^{\otimes 2} (\mathbb{S}_{AA'}) \right], \end{aligned} \quad (17)$$

where,  $\mathcal{U}_{\beta,t} := \mathcal{V}_\beta \circ \mathcal{U}_t$  with  $\mathcal{V}_\beta(X) := \exp[-\beta H/4] X \exp[-\beta H/4]$  the imaginary time-evolution,  $\mathcal{U}_t(X) := U_t^\dagger X U_t$  the real time-evolution, and  $U_t = \exp[-iHt]$  the usual time-evolution operator.

Consider a bipartite Hilbert space,  $\mathcal{H}_{AB} = \mathcal{H}_A \otimes \mathcal{H}_B$ . Let  $V \in \mathcal{U}(\mathcal{H}_A)$ ,  $W \in \mathcal{U}(\mathcal{H}_B)$  and  $\mathbb{E}_{U \in \mathcal{U}(\mathcal{H})} [f(U)]$  denote the Haar average of  $f(U)$  over  $\mathcal{U}(\mathcal{H})$ . Then, using the lemma [43],

$$\mathbb{E}_{U \in \mathcal{U}(\mathcal{H})} [U \otimes U^\dagger] = \frac{\mathbb{S}}{d}, \quad (\text{A1})$$

where  $\mathbb{S}$  is the swap operator on  $\mathcal{H} \otimes \mathcal{H}'$  with  $\mathcal{H}'$  representing a replica of the original Hilbert space  $\mathcal{H}$ . Given an orthonormal basis of  $\mathcal{H}$ ,  $\mathbb{B} = \{|j\rangle\}_{j=1}^d$  (and a replica of the basis for  $\mathcal{H}'$ ), the swap operator can be represented as  $\mathbb{S} = \sum_{j,k=1}^d |j\rangle\langle k| \otimes |k\rangle\langle j|$ . Now, if we consider Haar averages over a subsystem instead, then the lemma above is modified as,

$$\mathbb{E}_{V \in \mathcal{U}(\mathcal{H}_A)} V^\dagger \otimes V = \frac{\mathbb{S}_{AA'}}{d_A} \text{ and } \mathbb{E}_{W \in \mathcal{U}(\mathcal{H}_B)} W^\dagger \otimes W = \frac{\mathbb{S}_{BB'}}{d_B}. \quad (\text{A2})$$

First, we compute the disconnected BROTOC,

$$G_\beta^{(d)} := \mathbb{E}_{V \in \mathcal{U}(\mathcal{H}_A), W \in \mathcal{U}(\mathcal{H}_B)} F_\beta^{(d)} \quad (\text{A3})$$

$$= \mathbb{E}_{V \in \mathcal{U}(\mathcal{H}_A), W \in \mathcal{U}(\mathcal{H}_B)} \text{Tr} [(\sqrt{\rho_\beta} \otimes \sqrt{\rho_\beta}) (W^\dagger \otimes W) \mathbb{S}] \text{Tr} [(\sqrt{\rho_\beta} \otimes \sqrt{\rho_\beta}) (V^\dagger \otimes V) \mathbb{S}] \quad (\text{A4})$$

$$= \frac{1}{d} \text{Tr} [\mathbb{S} (\sqrt{\rho_\beta})^{\otimes 2} \mathbb{S}_{BB'}] \text{Tr} [\mathbb{S} (\sqrt{\rho_\beta})^{\otimes 2} \mathbb{S}_{AA'}] = \frac{1}{d} \text{Tr} [(\sqrt{\rho_\beta})^{\otimes 2} \mathbb{S}_{AA'}] \text{Tr} [(\sqrt{\rho_\beta})^{\otimes 2} \mathbb{S}_{BB'}], \quad (\text{A5})$$

where in the second line, we have used the lemma,  $\text{Tr}[(A \otimes B) \mathbb{S}] = \text{Tr}[AB]$  and in the third line we have used  $\mathbb{S} = \mathbb{S}_{AA'} \mathbb{S}_{BB'}$ ,  $\mathbb{S}^2 = \mathbb{I}$ ,  $\mathbb{S}_{AA'}^2 = \mathbb{I}_{AA'}$ , and  $\mathbb{S}_{BB'}^2 = \mathbb{I}_{BB'}$ .

We can formally perform partial traces above, for example,

$$\text{Tr} [(\sqrt{\rho_\beta} \otimes \sqrt{\rho_\beta}) \mathbb{S}_{AA'}] = \text{Tr}_{AA'} [\text{Tr}_{BB'} [(\sqrt{\rho_\beta} \otimes \sqrt{\rho_\beta})] S_{AA'}] = \text{Tr}_{AA'} [\sigma_A \otimes \sigma_{A'} \mathbb{S}_{AA'}] = \text{Tr} [\sigma_A^2], \quad (\text{A6})$$

where  $\sigma_A \equiv \text{Tr}_B [\sqrt{\rho_\beta}]$  above for brevity. Let  $\mathcal{P}_\chi(\rho) := \|\rho_\chi\|_2^2$  be the squared 2-norm of the operator  $\rho_\chi$  with  $\rho_\chi := \text{Tr}_{\overline{\chi}} [\rho]$  and  $\chi = \{A, B\}$  with  $\overline{\chi}$  the complement of  $\chi$ . Then,

$$G_d(\beta) = \frac{1}{d} \mathcal{P}_A(\sqrt{\rho_\beta}) \mathcal{P}_B(\sqrt{\rho_\beta}). \quad (\text{A7})$$

Similarly, for the connected BROTOC we have,

$$G_\beta^{(r)}(t) := \mathbb{E}_{V \in \mathcal{U}(\mathcal{H}_A), W \in \mathcal{U}(\mathcal{H}_B)} F_\beta^{(r)}(t) \quad (\text{A8})$$

$$= \mathbb{E}_{V \in \mathcal{U}(\mathcal{H}_A), W \in \mathcal{U}(\mathcal{H}_B)} \text{Tr} [\mathbb{S} (W_t^\dagger \otimes W_t) (y \otimes y) (V^\dagger \otimes V) (y \otimes y)] \quad (\text{A9})$$

$$= \frac{1}{d} \text{Tr} [\mathbb{S}_{AA'} y^{\otimes 2} U_t^{\dagger \otimes 2} S_{AA'} U_t^{\otimes 2} y^{\otimes 2}] \quad (\text{A10})$$

$$= \frac{1}{d\mathcal{Z}(\beta)} \text{Tr} [\mathbb{S}_{AA'} \mathcal{U}_{\beta,t}^{\otimes 2} (\mathbb{S}_{AA'})], \quad (\text{A11})$$

where  $\mathcal{U}_{\beta,t} := \mathcal{V}_\beta \circ \mathcal{U}_t$  with  $\mathcal{V}_\beta(X) := \exp[-\beta H/4] X \exp[-\beta H/4]$  the imaginary time-evolution,  $\mathcal{U}_t(X) := U_t^\dagger X U_t$  the real time-evolution, and  $U_t = \exp[-iHt]$  the usual time-evolution operator. This completes the proof.

## Proof of Proposition 4

**Proposition 4.**

$$\overline{G_\beta^{(r)}(t)} = \frac{1}{d\mathcal{Z}(\beta)} \left[ \sum_{j,k=1}^d \exp[-\beta(E_j + E_k)/2] \right. \\ \left. \left( |R_{jk}^A|^2 + |R_{jk}^B|^2 - \delta_{jk} |R_{jk}^A|^2 \right) \right]. \quad (37)$$

Recall that NRC implies nondegeneracy of the spectrum, therefore, using the spectral decomposition of a Hamiltonian,  $H = \sum_{j=1}^d E_j \Pi_j$  with  $\Pi_j = |\phi_j\rangle\langle\phi_j|$ , we have,

$$\mathcal{U}_{\beta,t}^{\otimes 2}(A) = \sum_{j,k,l,m}^d \exp[-\beta/4(E_j + E_k + E_l + E_m) - it(E_j + E_k - E_l - E_m)] (\Pi_j \otimes \Pi_k) A (\Pi_l \otimes \Pi_m). \quad (A12)$$

Using the NRC assumption, we have the following,  $\overline{\exp[-it(E_j + E_k - E_l - E_m)]}^t = \delta_{jl}\delta_{km} + \delta_{jm}\delta_{kl} - \delta_{jk}\delta_{kl}\delta_{lm}$ . Therefore,

$$\overline{G_\beta^{(r)}(t)} = \frac{1}{d\mathcal{Z}(\beta)} \left( \sum_{j,k}^d \exp[-\beta/2(E_j + E_k)] \text{Tr}[(\Pi_j \otimes \Pi_k) \mathbb{S}_{AA'} (\Pi_j \otimes \Pi_k) \mathbb{S}_{AA'}] \right. \quad (A13)$$

$$+ \sum_{j,k}^d \exp[-\beta/2(E_j + E_k)] \text{Tr}[(\Pi_j \otimes \Pi_k) \mathbb{S}_{BB'} (\Pi_j \otimes \Pi_k) \mathbb{S}_{BB'}] \quad (A14)$$

$$\left. - \sum_j^d \exp[-\beta E_j] \text{Tr}[\Pi_j^{\otimes 2} \mathbb{S}_{AA'} \Pi_j^{\otimes 2} \mathbb{S}_{AA'}] \right). \quad (A15)$$

Now, for pure states  $\Pi_j, \Pi_k$  one can show that  $\text{Tr}[(\Pi_j \otimes \Pi_k) \mathbb{S}_{AA'} (\Pi_j \otimes \Pi_k) \mathbb{S}_{AA'}] = |\text{Tr}[(\Pi_j \otimes \Pi_k) \mathbb{S}_{AA'}]|^2$ .

We now define the  $R$ -matrix introduced in Ref. [35] while computing the infinite-temperature variant of this Proposition. Let  $\rho_j^{A(B)} := \text{Tr}_{A(B)}[\Pi_j]$  be the reduced state, then, formally performing the partial trace we have,

$$\text{Tr}_{AA'BB'}[\Pi_k \otimes \Pi_l S_{AA'}] = \text{Tr}_{AA'}[\text{Tr}_{BB'}[\Pi_k \otimes \Pi_l] S_{AA'}] = \text{Tr}_{AA'}[\rho_k^A \otimes \rho_l^{A'} S_{AA'}] = \text{Tr}[\rho_k^A \rho_l^A] =: R_{kl}^A. \quad (A16)$$

Therefore, the time-average can be simplified as,

$$\overline{G_\beta^{(r)}(t)} = \frac{1}{d\mathcal{Z}(\beta)} \left( \sum_{j,k}^d \exp[-\beta/2(E_j + E_k)] \left( |R_{jk}^A|^2 + |R_{jk}^B|^2 - \delta_{jk} |R_{jk}^A|^2 \right) \right). \quad (A17)$$

Now we introduce a more compact notation for the equilibration value. Let  $\tilde{R}_{jk}^\chi := \exp[-\beta(E_j + E_k)/4] \langle \rho_j^\chi, \rho_k^\chi \rangle$ , then,

$$\overline{G_\beta^{(r)}(t)} = \frac{1}{d\mathcal{Z}(\beta)} \sum_{\chi \in \{A,B\}} \left( \left\| \tilde{R}^{(\chi)} \right\|_2^2 - \frac{1}{2} \left\| \tilde{R}_D^{(\chi)} \right\|_2^2 \right), \quad (A18)$$

with  $[\tilde{R}_D^{(\chi)}]_{jk} = [\tilde{R}_D^{(\chi)}]_{jk} \delta_{jk}$ ; where we have used the fact that  $R_{kk}^A = R_{kk}^B$ , that is, the the reduced states  $\rho_j^A$  and  $\rho_j^B$  are isospectral (up to irrelevant zeros).

## Proof of Proposition 5

**Proposition 5.** *For a symmetric bipartition of the Hilbert space,  $d_A = d_B = \sqrt{d}$  if  $\mathcal{P}(|\psi_{AB}\rangle) - \mathcal{P}_{\min} \leq \epsilon$  holds for all eigenstates, then for systems satisfying NRC, the equilibration value is bounded away from the maximally entangled case as follows,  $\left| \overline{G_\beta^{(r)}(t)}|_{\text{ME}} - \overline{G_\beta^{(r)}(t)}|_{\text{NRC}} \right| \leq \frac{\mathcal{Z}(\beta/2)^2}{d\mathcal{Z}(\beta)} \left( \frac{6\epsilon}{\sqrt{d}} + 3\epsilon^2 \right)$ .*

We prove this for the general case  $d_A \neq d_B$ , and the original Proposition can be recovered by setting  $d_A = d_B$  at the end. Let us assume without loss of generality that  $d_A \leq d_B$ . The spectral decomposition of the Hamiltonian is  $H = \sum_{j=1}^d E_j |\phi_j\rangle\langle\phi_j|$  and its reduced states are labelled as  $\rho_j^A := \text{Tr}_B [|\phi_j\rangle\langle\phi_j|]$ .

Notice that since  $\mathcal{P}(|\psi_{AB}\rangle) - \mathcal{P}_{\min} = \text{Tr} [\rho_A^2] - \frac{1}{d_A}$ , the assumption that the purities are nearly minimum can be equivalently expressed as:  $\mathcal{P}(\rho_k^A) - \mathcal{P}_{\min} \leq \epsilon \iff \|\Delta_k^A\|_2^2 \leq \epsilon$  with  $\Delta_k^A := \rho_k^A - I/d_A \quad \forall k$ .

Define  $\Delta_k^B$  analogously, i.e.,  $\Delta_k^B := \rho_k^B - I/d_B$ . Then, using the fact that the reduced states of a pure state are isospectral (therefore,  $\mathcal{P}(\rho_k^A) = \mathcal{P}(\rho_k^B) \quad \forall k$ ) and  $d_A \leq d_B$ , we have,  $\|\Delta_k^B\|_2^2 = \|\rho_k^B\|_2^2 - \frac{1}{d_B} = \|\rho_k^A\|_2^2 - \frac{1}{d_B} \leq \|\rho_k^A\|_2^2 - \frac{1}{d_A} \leq \epsilon \quad \forall k$ .

Now, recall that,  $\overline{G_\beta^{(r)}(t)}|_{\text{ME}} = \frac{1}{d^2} \left( \frac{2\mathcal{Z}(\beta/2)^2}{\mathcal{Z}(\beta)} - 1 \right)$  and  $\overline{G_\beta^{(r)}(t)} = \frac{1}{d\mathcal{Z}(\beta)} \left( \|\tilde{R}^A\|_2^2 + \|\tilde{R}^B\|_2^2 - \|\tilde{R}_D^A\|_2^2 \right)$ , where we have used the fact that  $\|\tilde{R}_D^{(A)}\|_2^2 = \|\tilde{R}_D^{(B)}\|_2^2$ . Then,

$$\left| \overline{G_\beta^{(r)}(t)}|_{\text{ME}} - \overline{G_\beta^{(r)}(t)}|_{\text{NRC}} \right| = \left| \frac{1}{d^2} \left( \frac{2\mathcal{Z}^2(\beta/2)}{\mathcal{Z}(\beta)} - 1 \right) - \frac{1}{d\mathcal{Z}(\beta)} \left( \|\tilde{R}^A\|_2^2 + \|\tilde{R}^B\|_2^2 - \|\tilde{R}_D^A\|_2^2 \right) \right| \quad (\text{A19})$$

$$\leq \underbrace{\left| \frac{1}{d^2\mathcal{Z}(\beta)} \mathcal{Z}^2(\beta/2) - \frac{1}{d\mathcal{Z}(\beta)} \|\tilde{R}^A\|_2^2 \right|}_{(i)} + \underbrace{\left| \frac{1}{d^2\mathcal{Z}(\beta)} \mathcal{Z}^2(\beta/2) - \frac{1}{d\mathcal{Z}(\beta)} \|\tilde{R}^B\|_2^2 \right|}_{(ii)} + \underbrace{\left| \frac{1}{d\mathcal{Z}(\beta)} \|\tilde{R}_D^A\|_2^2 - \frac{1}{d^2} \right|}_{(iii)}, \quad (\text{A20})$$

where we have split the terms in  $\overline{G_\beta^{(r)}(t)}|_{\text{ME}}$  and then used the triangle inequality. We now want to bound each of the terms (i), (ii), and (iii).

Since  $\|\tilde{R}^{(\chi)}\|_2^2 = \sum_{j,k=1}^d \exp[-\beta(E_j + E_k)/2] \left( \langle \rho_j^{(\chi)}, \rho_k^{(\chi)} \rangle \right)^2$  (note that we do not need an absolute value here since the exponential term is nonnegative and  $A, B \geq 0 \implies \langle A, B \rangle \geq 0$  so the inner products between the reduced states is nonnegative as well); we need to bound  $\left( \langle \rho_j^{(\chi)}, \rho_k^{(\chi)} \rangle \right)^2$ . Note that,

$$\left( \langle \rho_k^{(\chi)}, \rho_l^{(\chi)} \rangle \right)^2 = \left( \langle I/d_\chi + \Delta_k^{(\chi)}, I/d_\chi + \Delta_l^{(\chi)} \rangle \right)^2 = \left( \frac{1}{d_\chi} + \langle \Delta_k^{(\chi)}, \Delta_l^{(\chi)} \rangle \right)^2 = \frac{1}{d_\chi^2} + \frac{2}{d_\chi} \langle \Delta_k^{(\chi)}, \Delta_l^{(\chi)} \rangle + \langle \Delta_k^{(\chi)}, \Delta_l^{(\chi)} \rangle^2. \quad (\text{A21})$$

And, using Cauchy-Schwarz inequality along with the fact that  $\langle \Delta_k^{(\chi)}, \Delta_k^{(\chi)} \rangle = \|\rho_k^{(\chi)}\|_2^2 - \frac{1}{d_\chi} \leq \epsilon \quad \forall k$  (as shown above), we have,  $\langle \Delta_k^{(\chi)}, \Delta_l^{(\chi)} \rangle \leq \sqrt{\langle \Delta_k^{(\chi)}, \Delta_k^{(\chi)} \rangle \langle \Delta_l^{(\chi)}, \Delta_l^{(\chi)} \rangle} \leq \epsilon \quad \forall k, l$ . Therefore,  $\left( \langle \rho_k^{(\chi)}, \rho_l^{(\chi)} \rangle \right)^2 \leq \frac{1}{d_\chi^2} + \frac{2\epsilon}{d_\chi} + \epsilon^2 \equiv f(d_\chi, \epsilon) \quad \forall k, l$ .

Plugging this back in  $\|\tilde{R}^{(\chi)}\|_2^2$ , we have,  $\|\tilde{R}^{(\chi)}\|_2^2 = \sum_{j,k=1}^d \exp[-\beta(E_j + E_k)/2] f(d_\chi, \epsilon) = \mathcal{Z}(\beta/2)^2 f(d_\chi, \epsilon)$ . Now, for the diagonal part,  $\|\tilde{R}_D^A\|_2^2 = \sum_{j=1}^d \exp[-\beta E_j] (\langle \rho_j^A, \rho_j^A \rangle)^2 \leq \sum_{j=1}^d \exp[-\beta E_j] f(d_A, \epsilon) = \mathcal{Z}(\beta) f(d_A, \epsilon)$ .

Therefore, term (i) above becomes  $\frac{\mathcal{Z}^2(\beta/2)}{d\mathcal{Z}(\beta)} \left| \frac{1}{d} - f(d_A, \epsilon) \right|$  and term (ii) becomes,  $\frac{\mathcal{Z}^2(\beta/2)}{d\mathcal{Z}(\beta)} \left| \frac{1}{d} - f(d_B, \epsilon) \right|$ . And, term (iii) becomes,  $\frac{1}{d} \left| \frac{1}{d} - f(d_A, \epsilon) \right|$ . Now, notice that

$$\mathcal{Z}(\beta/2)^2 = \sum_{j,k=1}^d \exp[-\beta E_j/2] \exp[-\beta E_k/2] = \sum_{j=k}^d \exp[-\beta E_j/2] \exp[-\beta E_k/2] \quad (\text{A22})$$

$$+ \sum_{j \neq k}^d \exp[-\beta E_j/2] \exp[-\beta E_k/2] \geq \sum_{j=1}^d \exp[-\beta E_j] = \mathcal{Z}(\beta), \quad (\text{A23})$$

where we have dropped the  $j \neq k$  terms in the summation and used their nonnegativity. Therefore,  $\mathcal{Z}(\beta/2)^2/\mathcal{Z}(\beta) \geq 1$  and so, term (iii) can be upper bounded as  $\frac{1}{d} \left| \frac{1}{d} - f(d_A, \epsilon) \right| \leq \frac{\mathcal{Z}(\beta/2)^2}{d\mathcal{Z}(\beta)} \left| \frac{1}{d} - f(d_A, \epsilon) \right|$ .

Putting everything together, we have

$$\left| \overline{G_\beta^{(r)}(t)}|_{\text{ME}} - \overline{G_\beta^{(r)}(t)}|_{\text{NRC}} \right| \leq \frac{\mathcal{Z}(\beta/2)^2}{d\mathcal{Z}(\beta)} \left( 2 \left| \frac{1}{d} - f(d_A, \epsilon) \right| + \left| \frac{1}{d} - f(d_B, \epsilon) \right| \right). \quad (\text{A24})$$

Now, if we set  $d_A = d_B = \sqrt{d}$ , we have,  $\left| \frac{1}{d} - f(d_A, \epsilon) \right| = \left| \frac{1}{d} - \left( \frac{1}{d} + \frac{2\epsilon}{\sqrt{d}} + \epsilon^2 \right) \right| = \left( \frac{2\epsilon}{\sqrt{d}} + \epsilon^2 \right)$ . Therefore,

$$\left| \overline{G_\beta^{(r)}(t)}|_{\text{ME}} - \overline{G_\beta^{(r)}(t)}|_{\text{NRC}} \right| \leq \frac{\mathcal{Z}(\beta/2)^2}{d\mathcal{Z}(\beta)} \left( \frac{6\epsilon}{\sqrt{d}} + 3\epsilon^2 \right). \quad (\text{A25})$$

## Proof of Proposition 2

**Proposition 2.** *The regularized four-point OTOC averaged globally over Haar-random unitaries is related to the four-point spectral form factor as,  $\mathbb{E}_{A_1, B_1, A_2 \in \mathcal{U}(\mathcal{H})} \left[ F_\beta^{(A_1, B_1, A_2, B_2)}(t) \right] = \mathcal{R}_4^{(H)}(\beta/4, t) / (d^3 \mathcal{Z}(\beta))$ , where  $B_2 = A_2^\dagger B_1^\dagger A_1^\dagger$  and  $\mathcal{R}_4^{(H)}(\beta, t) := (\mathcal{Z}_\beta(t) \mathcal{Z}_\beta(t)^*)^2$  with  $\mathcal{Z}_\beta(t) = \text{Tr} [\exp [(-\beta + it)H]]$ , the analytically continued partition function.*

We have,

$$F_\beta^{(A_1, B_1, A_2, B_2)}(t) = \frac{1}{\mathcal{Z}(\beta)} \text{Tr} \left[ x \mathcal{U}_t(A_1) x B_1 x \mathcal{U}_t(A_2) x \left( A_2^\dagger B_1^\dagger A_1^\dagger \right) \right], \quad (\text{A26})$$

where we have used  $B_2 = A_2^\dagger B_1^\dagger A_1^\dagger$ . Now, using the cyclicity of trace and the lemma  $\mathbb{E}_{A \in \mathcal{U}(\mathcal{H})} A X A^\dagger = \frac{\text{Tr}[X]}{d}$ , we have,

$$\mathbb{E}_{A_1 \in \mathcal{U}(\mathcal{H})} F_\beta^{(A_1, B_1, A_2, B_2)}(t) = \frac{1}{d\mathcal{Z}(\beta)} \text{Tr} \left[ x U_t^\dagger \right] \text{Tr} \left[ U_t x B_1 x \mathcal{U}_t(A_2) x \left( A_2^\dagger B_1^\dagger \right) \right] \quad (\text{A27})$$

$$= \frac{1}{d\mathcal{Z}(\beta)} \text{Tr} \left[ x U_t^\dagger \right] \text{Tr} \left[ B_1^\dagger U_t x B_1 x \mathcal{U}_t(A_2) x \left( A_2^\dagger \right) \right], \quad (\text{A28})$$

where in the second line we have used the cyclicity of trace to move  $B_1^\dagger$  to the front. Now, performing  $\mathbb{E}_{B_1}$  using the lemma above, we have,

$$\mathbb{E}_{B_1 \in \mathcal{U}(\mathcal{H})} \text{Tr} \left[ B_1^\dagger U_t x B_1 x \mathcal{U}_t(A_2) x \left( A_2^\dagger \right) \right] = \frac{1}{d} \text{Tr} [U_t x] \text{Tr} \left[ x U_t^\dagger A_2 U_t x A_2^\dagger \right]. \quad (\text{A29})$$

Similarly, performing the average over  $A_2$  we obtain the final terms that are proportional to  $\text{Tr} [U_t x] \text{Tr} [U_t^\dagger x]$ . Thus, we have the desired result.

## Unregularized OTOCs for maximally entangled models

Consider an operator Schmidt decomposition of  $U_t \equiv U = \sum_j \sqrt{\lambda_j} U_j \otimes W_j$  with  $U_j \in \mathcal{L}(\mathcal{H}_A)$  and  $W_j \in \mathcal{L}(\mathcal{H}_B)$  such that  $\langle U_j, U_k \rangle = d_A \delta_{jk}$  and  $\langle W_j, W_k \rangle = d_B \delta_{jk}$ . For a unitary operator,  $\|U\|_2^2 = d$ , therefore, we have,

$$\|U\|_2^2 = \text{Tr} \left[ \sum_{j,k} \sqrt{\lambda_j \lambda_k} U_j U_k^\dagger \otimes W_j W_k^\dagger \right] = \sum_{j,l} \sqrt{\lambda_j \lambda_k} \langle U_j, U_k \rangle \langle W_j, W_k \rangle = d_A d_B \sum_j \lambda_j \implies \sum_j \lambda_j = 1. \quad (\text{A30})$$

Now, consider the bipartite unregularized OTOC,  $F_\beta(U) = \frac{1}{d} \text{Tr} [(\rho_\beta \otimes \mathbb{I}) U^{\otimes 2} \mathbb{S}_{AA'} U^\dagger \otimes \mathbb{S}_{AA'}]$ . Plugging in the operator Schmidt decomposition of  $U$ , we have,

$$\begin{aligned} F_\beta(U) &= \frac{1}{d} \text{Tr} \left[ (\rho_\beta \otimes \mathbb{I}) \left( \sum_j \sqrt{\lambda_j} U_j \otimes W_j \right)^{\otimes 2} \mathbb{S}_{AA'} \left( \sum_k \sqrt{\lambda_k} U_k^\dagger \otimes W_k^\dagger \right)^{\otimes 2} \mathbb{S}_{AA'} \right]^{\otimes 2} \\ &= \frac{1}{d} \sum_{jklm} \sqrt{\lambda_j \lambda_k \lambda_l \lambda_m} \text{Tr} \left[ (\rho_\beta \otimes \mathbb{I}) (U_j \otimes W_j \otimes U_k \otimes W_k) \mathbb{S}_{AA'} (U_l^\dagger \otimes W_l^\dagger \otimes U_m^\dagger \otimes W_m^\dagger) \mathbb{S}_{AA'} \right] \\ &= \frac{1}{d} \sum_{jklm} \sqrt{\lambda_j \lambda_k \lambda_l \lambda_m} \text{Tr} \left[ (\rho_\beta \otimes \mathbb{I}) (U_j \otimes W_j \otimes U_k \otimes W_k) (U_m^\dagger \otimes W_l^\dagger \otimes U_l^\dagger \otimes W_m^\dagger) \right], \end{aligned}$$

where we have used the adjoint action  $\mathbb{S}_{AA'} (X_A \otimes Y_{A'}) \mathbb{S}_{AA'} = Y_A \otimes X_{A'}$ . Then,

$$F_\beta(U) = \sum_{jk} \sqrt{\lambda_j} (\lambda_k)^{3/2} \text{Tr} \left[ \rho_\beta (U_j \otimes W_j) (U_k^\dagger \otimes W_k^\dagger) \right], \quad (\text{A31})$$

where we have used the fact that  $\langle U_j, U_k \rangle = d_A \delta_{jk}$  and  $\langle W_j, W_k \rangle = d_B \delta_{jk}$  and summed over two of the indices of the summation above. Now, if  $U$  is maximally entangled (namely, its eigenstates are maximally entangled) across  $d_A = d_B = \sqrt{d}$  and one has  $\sqrt{\lambda_j} = \sqrt{\frac{1}{d_A^2}}$ , then

$$F_\beta(U) = \frac{1}{d_A^2} \text{Tr} \left[ \rho_\beta \left( \sum_j \sqrt{\lambda_j} U_j \otimes W_j \right) \left( \sum_k \sqrt{\lambda_j} U_k \otimes W_k \right) \right] = \frac{1}{d_A^2} \text{Tr} [\rho_\beta U U^\dagger] = \frac{1}{d_A^2}. \quad (\text{A32})$$

Therefore,  $G_\beta(U) = 1 - F_\beta(U) = 1 - \frac{1}{d_A^2}$  and is independent of  $\beta$ .

### The dynamical map $\mathcal{U}_{\beta,t}$ is a quantum operation

Recall that the Choi-Jamiolkowski (CJ) isomorphism is an isomorphism between linear maps  $\mathcal{E} : \mathcal{L}(\mathcal{H}) \rightarrow \mathcal{L}(\mathcal{K})$  to matrices  $\rho_{\mathcal{E}} \in \mathcal{L}(\mathcal{H}) \otimes \mathcal{L}(\mathcal{K})$ . Let  $|\phi^+\rangle := \frac{1}{\sqrt{d}} |j\rangle |j\rangle$  be the *normalized* maximally entangled state in  $\mathcal{H}^{\otimes 2}$ , then,

$$\rho_{\mathcal{E}} := \mathcal{E} \otimes \mathcal{I} (|\phi^+\rangle \langle \phi^+|). \quad (\text{A33})$$

A linear map  $\mathcal{E}$  is CP  $\iff \rho_{\mathcal{E}} \geq 0$ . Computing the CJ matrix corresponding to the linear map  $\mathcal{V}_\beta(X) := \exp[-\beta H/4] X \exp[-\beta H/4]$ , we have,

$$\rho_{\mathcal{V}_\beta} = \frac{1}{d} \sum_{j,k=1}^d \mathcal{V}_\beta \otimes \mathcal{I} (|j\rangle \langle k| \otimes |j\rangle \langle k|) \quad (\text{A34})$$

$$= \frac{1}{d} \sum_{j,k=1}^d \exp[-\beta (E_j + E_k)/4] (|j\rangle \langle k| \otimes |j\rangle \langle k|) = \frac{\mathcal{Z}(\beta/2)}{d} |\psi(\beta/2)\rangle \langle \psi(\beta/2)|, \quad (\text{A35})$$

where in the second equality we have used the expansion of the TDS Eq. (19). Now, since  $|\psi(\beta/2)\rangle \langle \psi(\beta/2)|$  is a pure state (or a rank-1 projector), it is positive semidefinite. Moreover,  $\frac{\mathcal{Z}(\beta/2)}{d} \geq 0$ , therefore,  $\rho_{\mathcal{V}_\beta} \geq 0$ . As a result,  $\mathcal{V}_\beta$  is a CP map.

To show that the map  $\mathcal{V}_\beta$  is trace-nonincreasing, we have to show that  $\text{Tr} [\mathcal{V}_\beta(\rho)] \leq \text{Tr} [\rho] \quad \forall \rho \in \mathcal{B}(\mathcal{H})$ . Namely,

$$\iff \text{Tr} [\mathcal{V}_\beta(\rho) - \rho] \leq 0 \quad \forall \rho, \quad (\text{A36})$$

$$\iff \text{Tr} [\exp[-\beta H/4] \rho \exp[-\beta H/4] - \rho] \leq 0 \quad \forall \rho \quad (\text{A37})$$

$$\iff \text{Tr} [(\exp[-\beta H/2] - \mathbb{I}) \rho] \leq 0 \quad \forall \rho, \quad (\text{A38})$$

$$\iff \exp[-\beta H/2] \leq \mathbb{I}, \quad (\text{A39})$$

where in the last line, we have used the definition of positive semidefiniteness. Now, assuming  $H \geq 0$ , we have,  $\exp[-\beta H/2] \leq \mathbb{I}$  since  $\exp[-\beta E_j/2] \leq 1$  if  $\beta, E_j \geq 0 \quad \forall j$ . Notice that, the matrix  $\rho_{\mathcal{V}_\beta}$  is *subnormalized* with  $\text{Tr} [\rho_{\mathcal{V}_\beta}] = \frac{\mathcal{Z}(\beta/2)}{d} \leq 1$ . Therefore, the dynamical map,  $\mathcal{V}_\beta$  is a CP and trace-nonincreasing linear map, that is, it is a physical quantum operation [49] and we can think of  $\rho_{\mathcal{V}_\beta}$  as a subnormalized density matrix corresponding to a quantum process [105, 106].

### Equilibration value of NRC-PS

To compute the equilibration value, we need to evaluate the  $R$ -matrix. Recall that  $H_{\text{NRC-PS}} := \sum_{j,k=1}^{d_A, d_B} E_{j,k} |\phi_j^{(A)}\rangle \langle \phi_j^{(A)}| \otimes |\phi_k^{(B)}\rangle \langle \phi_k^{(B)}|$ , with the additional assumption that the spectrum  $\{E_{j,k}\}_{j,k}$  satisfies

NRC. Define the index  $\alpha \equiv (j, k)$  with  $\alpha \in \{1, 2, \dots, d\}$  and  $j \in \{1, 2, \dots, d_A\}, k \in \{1, 2, \dots, d_B\}$ . Then,

$\rho_\alpha^A = \text{Tr}_B [\rho_\alpha] = \text{Tr}_B [\rho_{jk}] = |\phi_j^A\rangle \langle \phi_j^A|$ , that is for all paired indices  $(j, k)$  and  $(j, k')$  the reduced states are the same. For the  $R$ -matrix, consider  $\alpha = (j, k)$  and  $\beta = (l, m)$ , we have,  $R_{\alpha,\beta}^A = \langle \rho_\alpha^A, \rho_\beta^A \rangle = \delta_{j,l}$ . Similarly, we have,  $\rho_\alpha^B = \text{Tr}_A [\rho_\alpha] = \text{Tr}_A [\rho_{jk}] = |\phi_k^B\rangle \langle \phi_k^B|$  and  $R_{\alpha,\beta}^B = \delta_{k,m}$ .

We are now ready to evaluate  $\overline{G_\beta^{(r)}(t)}$ . Notice that

$$\sum_{\alpha,\beta=1}^d \exp[-\beta/2(E_\alpha + E_\beta)] |R_{\alpha,\beta}^A|^2 = \sum_{j,k,l,m=1}^{d_A, d_B} \exp[-\beta/2(E_{j,k} + E_{l,m})] |\delta_{j,l}|^2 \quad (\text{A40})$$

$$= \sum_{j,k,m=1}^{d_A, d_B, d_B} \exp[-\beta/2(E_{j,k} + E_{j,m})] = \sum_{j=1}^{d_A} \left( \sum_{k=1}^{d_B} \exp[-\beta E_{j,k}/2] \right)^2. \quad (\text{A41})$$

Defining,  $\Theta_j^A := \left( \sum_{k=1}^{d_B} \exp[-\beta E_{j,k}/2] \right)^2$ , we have,  $\sum_{\alpha,\beta=1}^d \exp[-\beta/2(E_\alpha + E_\beta)] |R_{\alpha,\beta}^A|^2 = \sum_{j=1}^{d_A} \Theta_j^A$ . Similar algebraic manipulations prove the final result,

$$\overline{G_\beta^{(r)}(t)} = \frac{1}{dZ(\beta)} \left( \sum_{j=1}^{d_A} \Theta_j^A + \sum_{k=1}^{d_B} \Theta_k^B - Z(\beta) \right). \quad (\text{A42})$$

This can then be rewritten in the form in the main text, namely,

$$\overline{G_\beta^{(r)}(t)}|_{\text{NRC-PS}} = \frac{1}{d} \left( \frac{\|\mathbf{p}^A(\beta/2)\|^2 + \|\mathbf{p}^B(\beta/2)\|^2}{\|\mathbf{p}(\beta/2)\|^2} - 1 \right), \quad (\text{A43})$$

where the probability vector  $\mathbf{p}(\beta)$  is defined by the components  $p_j = \frac{e^{-\beta E_j}}{Z(\beta)}$  and  $\mathbf{p}^{A/B}(\beta)$  are its marginals.

Moreover, for the disconnected correlator, a similar calculation shows that,

$$G_\beta^{(d)} = \frac{1}{dZ(\beta)^2} \left( \sum_{j=1}^{d_A} \Theta_j^A \right) \left( \sum_{k=1}^{d_B} \Theta_k^B \right). \quad (\text{A44})$$

## Numerical details

The  $R^2$  value for all linear fits was  $\gtrsim 0.99$  for all data and hence we do not report the numbers here.

Model	$\beta = 0$	$\beta = 1$	$\beta = \infty$
TFIM integrable	0.523785	0.0341617	-0.525957
NRC-PS	0.971448	0.83213	1.00
Anderson	1.13615	0.742852	$6.79567 \times 10^{-7}$
MBL	0.700658	0.213039	-0.012799
TFIM chaotic	1.60648	0.327334	-0.00502613
GUE	1.12868	2.56073	2.10215

**Table A1:** The  $\log_2(\alpha)$  for various Hamiltonian models at  $\beta = 0, 1, \infty$ , given the Ansatz  $\overline{G_\beta^{(r)}(t)} = \alpha d^{-\gamma}$ .